Developing a data-driven method to constrain the antiproton background in Mu2e

17^{th} International Workshop on Tau Lepton Physics
University of Louisville, Kentucky, USA

Namitha Chithirasreemadam*, Simone Donati*, Pavel Murat**

Università di Pisa, INFN Pisa*
Fermi National Accelerator Laboratory**

04 Dec 2023

namitha@pi.infn.it

H2020 MSCA ITN
G.A. 858199

Mu2e

- Search for neutrinoless, coherent conversion $\mu^- N \rightarrow e^- N$ in the field of an Aluminium nucleus by measuring,

$$R_{\mu e} = \frac{\Gamma(\mu^- + N(Z,A) \rightarrow e^- + N(Z,A))}{\Gamma(\mu^- + N(Z,A) \rightarrow \nu_\mu + N(Z-1,A))}$$

- Signal: Monochromatic conversion electron (CE) with energy $E_{CE} = m_\mu - E_{BE} - E_{recoil}$

  For the Al stopping target (ST), $E_{CE} = 104.97$ MeV*.

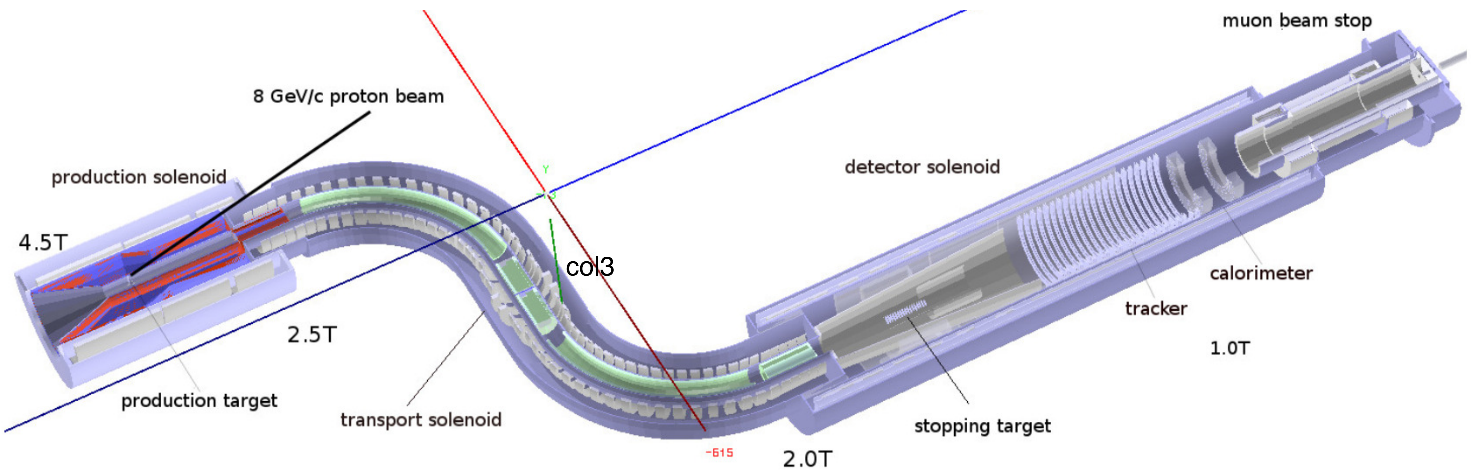

Production Solenoid (PS)	**Transport Solenoid (TS)**	**Detector Solenoid (DS)**
p beam interacts with the Tungsten target. Mostly produces pions.	Selects μ^- with p < 100 MeV/c. COL3 selects μ^-/μ^+ beam.	μ^- stop in the Al target. Annular tracker and calorimeter to detect CE.

*Czarnecki, i Tormo https://journals.aps.org/prd/pdf/10.1103/PhysRevD.84.013006

Background summary and expected sensitivity

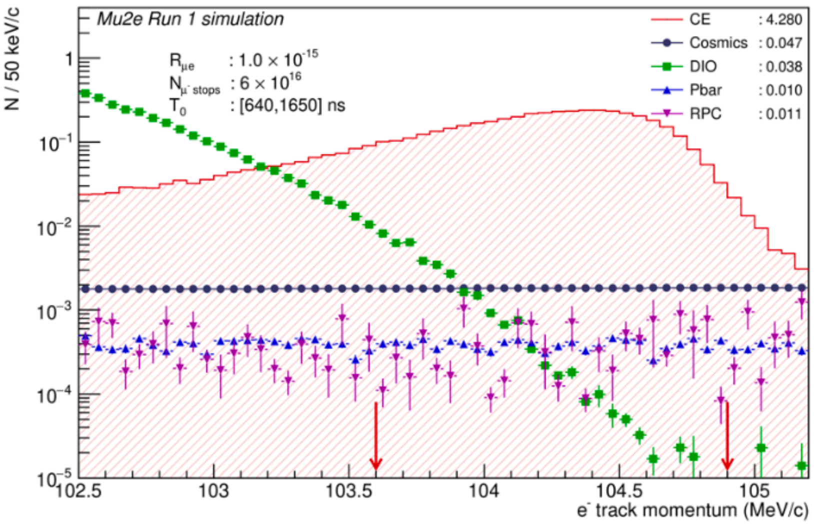

e^- momentum distribution after optimisation of the signal momentum and time window.

Channel	Mu2e Run I
SES	2.4×10^{-16}
Cosmics	0.046 ± 0.010 (stat) ± 0.009 (syst)
DIO	0.038 ± 0.002 (stat) $^{+0.025}_{-0.015}$ (syst)
Antiprotons	0.010 ± 0.003 (stat) ± 0.010 (syst)
RPC in-time	0.010 ± 0.002 (stat) $^{+0.001}_{-0.003}$ (syst)
RPC out-of-time ($\zeta = 10^{-10}$)	$(1.2 \pm 0.1$ (stat) $^{+0.1}_{-0.3}$ (syst)$) \times 10^{-3}$
RMC	$< 2.4 \times 10^{-3}$
Decays in flight	$< 2 \times 10^{-3}$
Beam electrons	$< 1 \times 10^{-3}$
Total	0.105 ± 0.032

Expected backgrounds in the signal momentum and time window [103.6-104.90 MeV/c], [640-1650 ns]*

Background summary and expected sensitivity

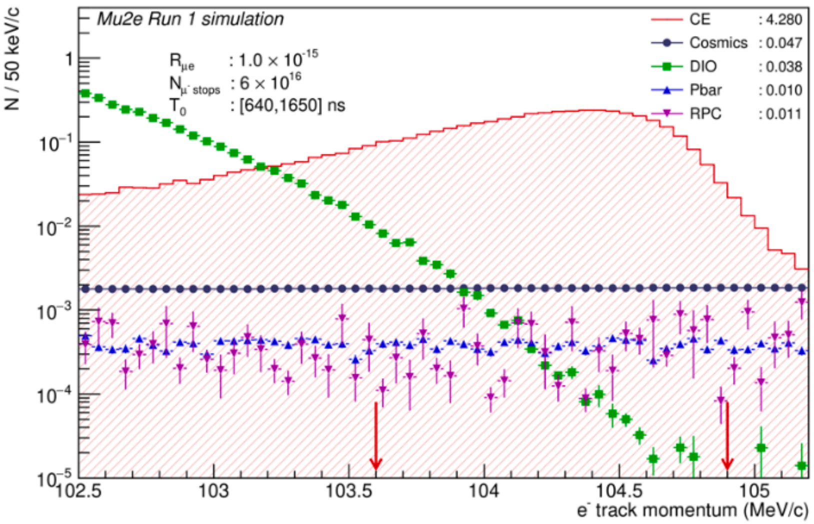

e^- momentum distribution after optimisation of the signal momentum and time window.

Channel	Mu2e Run I
SES	2.4×10^{-16}
Cosmics	0.046 ± 0.010 (stat) ±0.009 (syst)
DIO	0.038 ± 0.002 (stat) $^{+0.025}_{-0.015}$ (syst)
Antiprotons	0.010 ± 0.003 (stat) ±0.010 (syst)
RPC in-time	0.010 ± 0.002 (stat) $^{+0.001}_{-0.003}$ (syst)
RPC out-of-time ($\zeta=10^{-10}$)	$(1.2\pm0.1$ (stat) $^{+0.1}_{-0.3}$ (syst)$)\times10^{-3}$
RMC	$<2.4\times10^{-3}$
Decays in flight	$<2\times10^{-3}$
Beam electrons	$<1\times10^{-3}$
Total	0.105 ± 0.032

Expected backgrounds in the signal momentum and time window [103.6-104.90 MeV/c], [640-1650 ns]*

- The expected Run I 5σ discovery sensitivity is $R_{\mu e}=1.2\times10^{-15}$.

Background summary and expected sensitivity

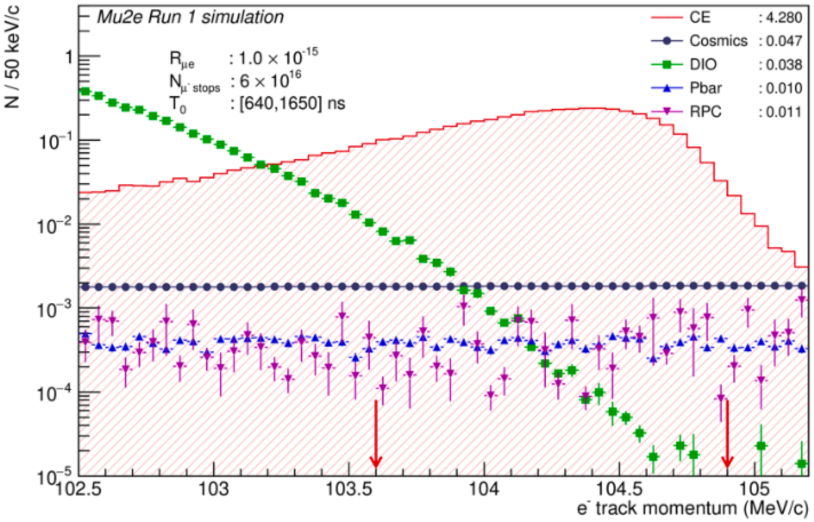

e^- momentum distribution after optimisation of the signal momentum and time window.

Channel	Mu2e Run I
SES	2.4×10^{-16}
Cosmics	0.046 ± 0.010 (stat) ± 0.009 (syst)
DIO	0.038 ± 0.002 (stat) $^{+0.025}_{-0.015}$ (syst)
Antiprotons	0.010 ± 0.003 (stat) ± 0.010 (syst)
RPC in-time	0.010 ± 0.002 (stat) $^{+0.001}_{-0.003}$ (syst)
RPC out-of-time ($\zeta = 10^{-10}$)	$(1.2 \pm 0.1$ (stat) $^{+0.1}_{-0.3}$ (syst)$) \times 10^{-3}$
RMC	$< 2.4 \times 10^{-3}$
Decays in flight	$< 2 \times 10^{-3}$
Beam electrons	$< 1 \times 10^{-3}$
Total	0.105 ± 0.032

Expected backgrounds in the signal momentum and time window [103.6-104.90 MeV/c], [640-1650 ns]*

- The expected Run I 5σ discovery sensitivity is $R_{\mu e} = 1.2 \times 10^{-15}$.
- If no signal, the expected upper limit is $R_{\mu e} < 6.2 \times 10^{-16}$ at 90% CL.

Background summary and expected sensitivity

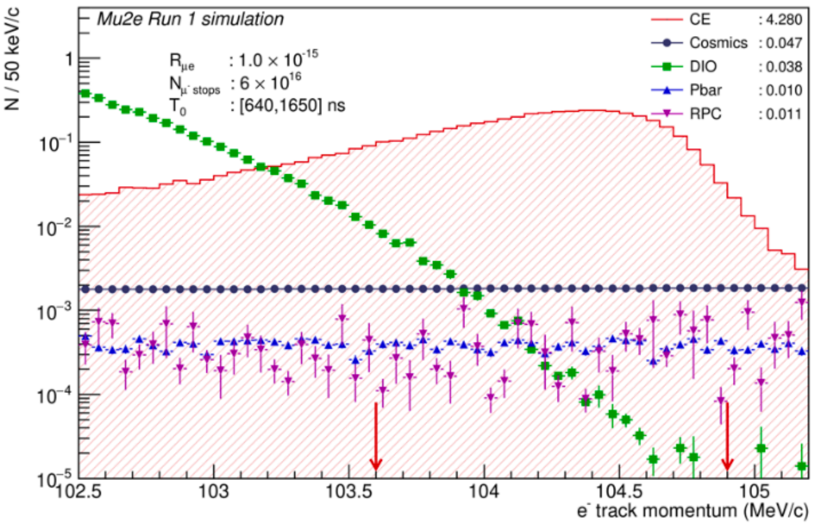

e^- momentum distribution after optimisation of the signal momentum and time window.

Channel	Mu2e Run I
SES	2.4×10^{-16}
Cosmics	0.046 ± 0.010 (stat) ± 0.009 (syst)
DIO	0.038 ± 0.002 (stat) $^{+0.025}_{-0.015}$ (syst)
Antiprotons	0.010 ± 0.003 (stat) ± 0.010 (syst)
RPC in-time	0.010 ± 0.002 (stat) $^{+0.001}_{-0.003}$ (syst)
RPC out-of-time ($\zeta = 10^{-10}$)	$(1.2 \pm 0.1$ (stat) $^{+0.1}_{-0.3}$ (syst)$) \times 10^{-3}$
RMC	$< 2.4 \times 10^{-3}$
Decays in flight	$< 2 \times 10^{-3}$
Beam electrons	$< 1 \times 10^{-3}$
Total	0.105 ± 0.032

Expected backgrounds in the signal momentum and time window [103.6-104.90 MeV/c], [640-1650 ns]*

- The expected Run I 5σ discovery sensitivity is $R_{\mu e} = 1.2 \times 10^{-15}$.
- If no signal, the expected upper limit is $R_{\mu e} < 6.2 \times 10^{-16}$ at 90% CL.
- The estimated $\overline{p}$ background for Run 1 is $0.010 \pm 0.003(stat) \pm 0.010(syst)$*.
  The systematic error is dominated by the uncertainty on the $\overline{p}$ production cross section.

*Mu2e Collaboration MDPI Universe 2023 https://doi.org/10.3390/universe9010054

Antiproton background in Mu2e

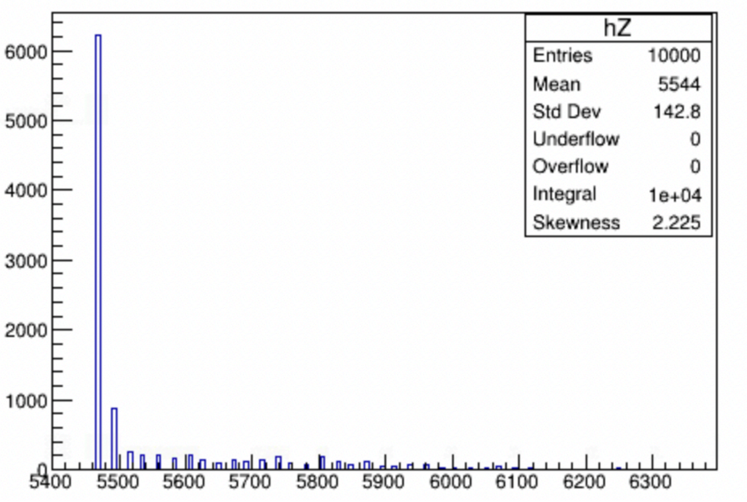

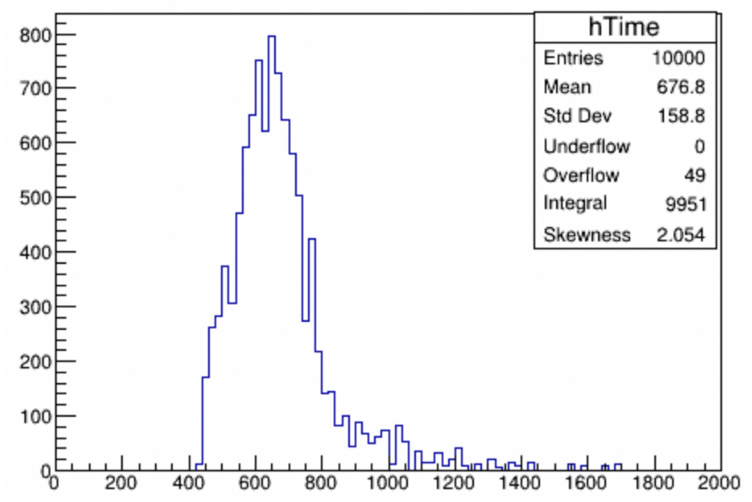

z (mm) from the centre of the TS
Longitudinal position of $\overline{p}$ annihilations

time (ns) of $\overline{p}$ annihilations
$\overline{p}'s$ stop within the live data taking window [640-1650 ns]

Antiproton background in Mu2e

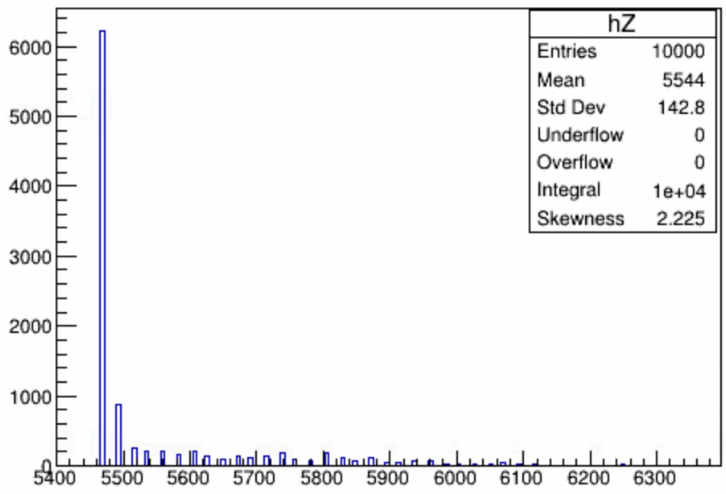

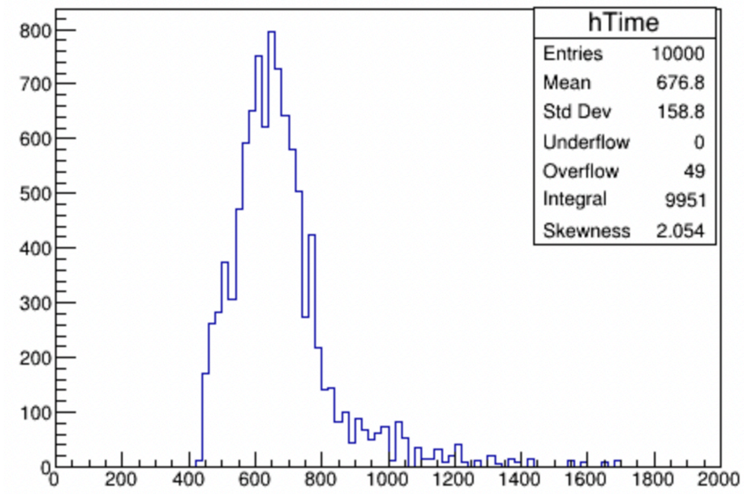

z (mm) from the centre of the TS
Longitudinal position of $\overline{p}$ annihilations

time (ns) of $\overline{p}$ annihilations
$\overline{p}'s$ stop within the live data taking window
[640-1650 ns]

- $\overline{p}'s$ are produced by the pW interactions in the PS.

Antiproton background in Mu2e

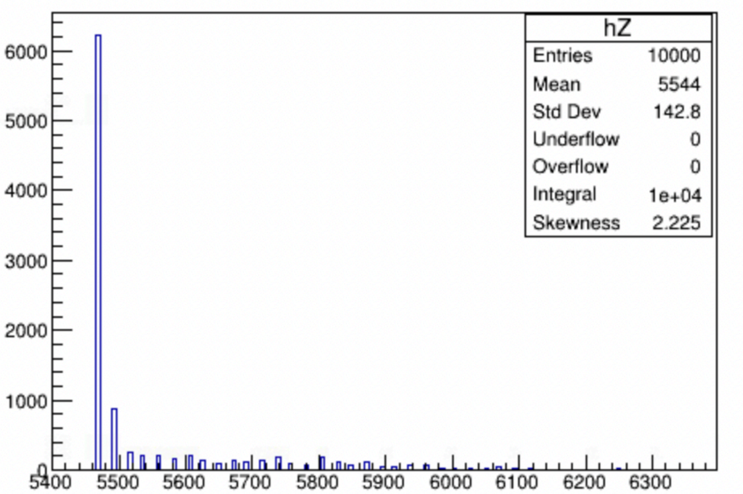

z (mm) from the centre of the TS
Longitudinal position of $\overline{p}$ annihilations

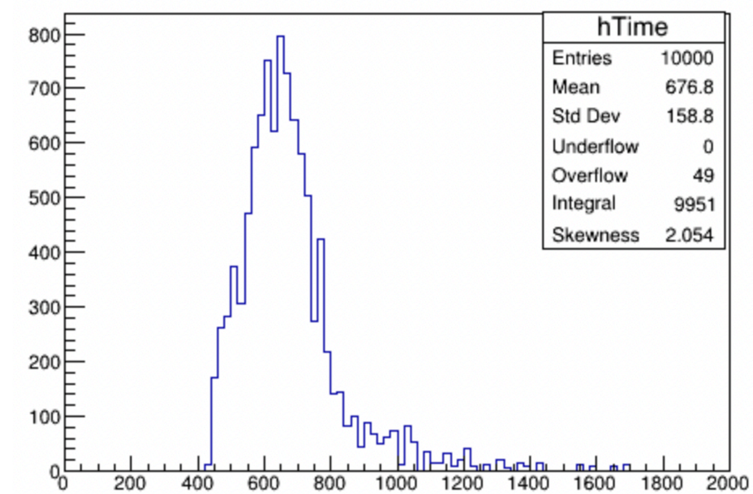

time (ns) of $\overline{p}$ annihilations
$\overline{p}'s$ stop within the live data taking window
[640-1650 ns]

- $\overline{p}'s$ are produced by the pW interactions in the PS.
- Very few $\overline{p}'s$ reach the DS, most of them stop within the first foil of the ST.

Antiproton background in Mu2e

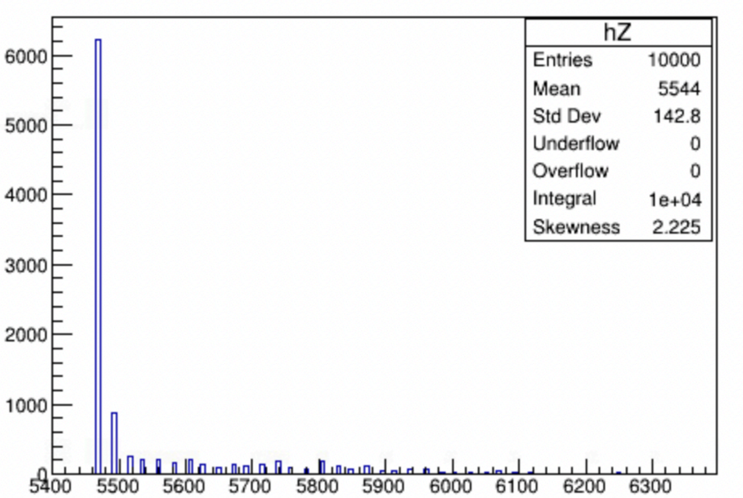

z (mm) from the centre of the TS
Longitudinal position of $\overline{p}$ annihilations

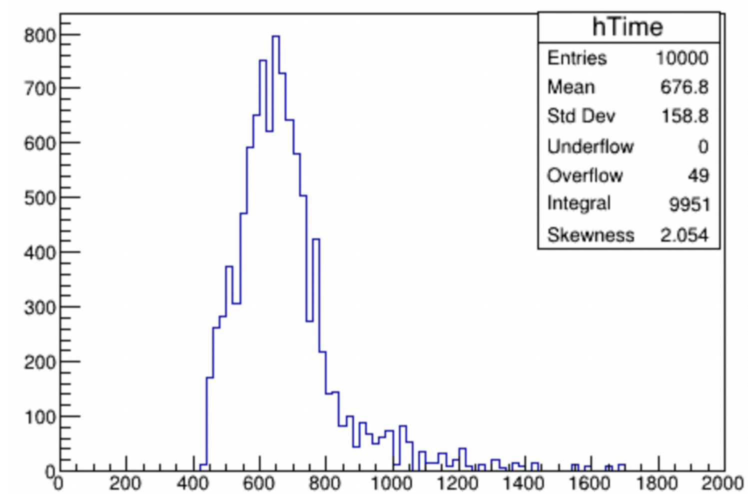

time (ns) of $\overline{p}$ annihilations
$\overline{p}'s$ stop within the live data taking window [640-1650 ns]

- $\overline{p}'s$ are produced by the pW interactions in the PS.
- Very few $\overline{p}'s$ reach the DS, most of them stop within the first foil of the ST.
- $p\overline{p}$ annihilation at the ST can produce e^- by $\pi^0 \to \gamma\gamma$ decays followed by γ conversions and $\pi^- \to \mu^-\overline{\nu}$ decays followed by μ^- decays.

Antiproton background in Mu2e

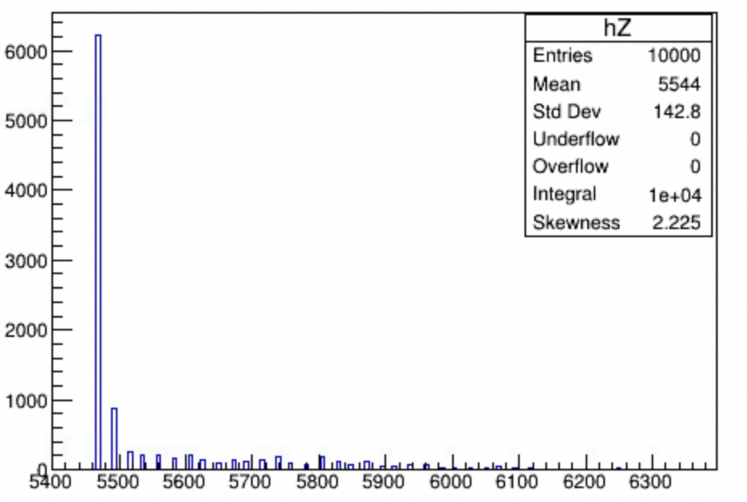

z (mm) from the centre of the TS
Longitudinal position of $\overline{p}$ annihilations

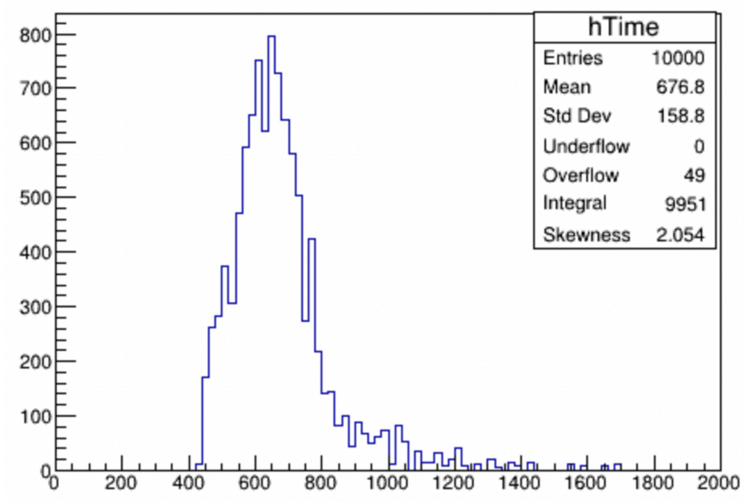

time (ns) of $\overline{p}$ annihilations
$\overline{p}'s$ stop within the live data taking window [640-1650 ns]

- $\overline{p}'s$ are produced by the pW interactions in the PS.
- Very few $\overline{p}'s$ reach the DS, most of them stop within the first foil of the ST.
- $p\overline{p}$ annihilation at the ST can produce e^- by $\pi^0 \to \gamma\gamma$ decays followed by γ conversions and $\pi^- \to \mu^-\overline{\nu}$ decays followed by μ^- decays.
- $p\overline{p}$ annihilation in the TS can cause delayed Radiative Pion Capture.

Antiproton background in Mu2e

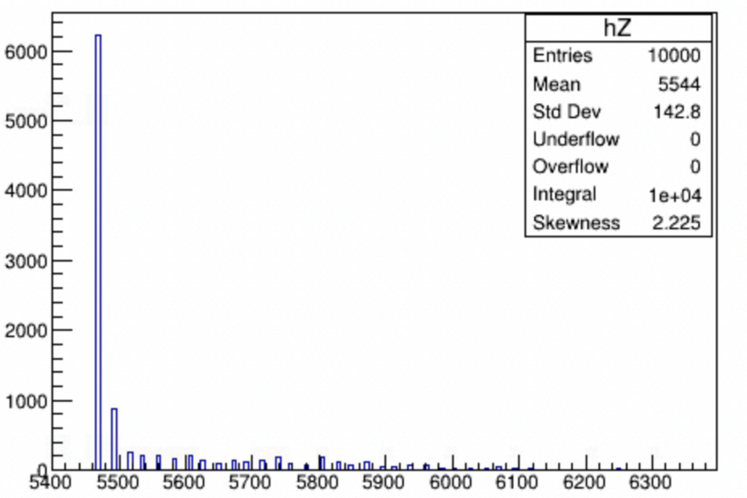

z (mm) from the centre of the TS
Longitudinal position of $\overline{p}$ annihilations

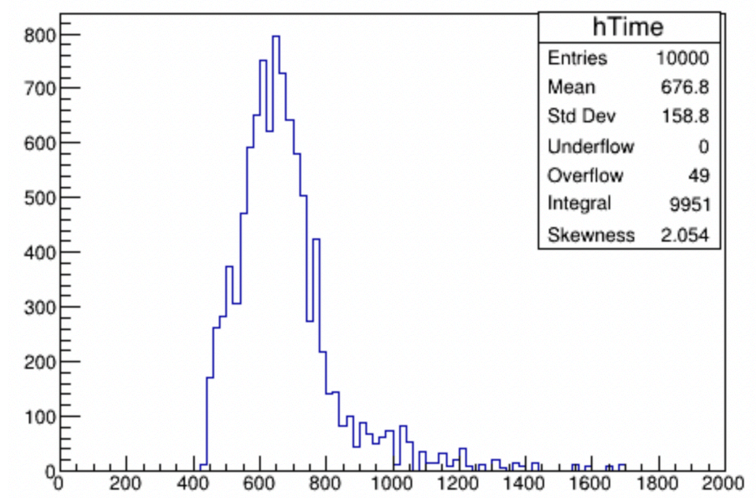

time (ns) of $\overline{p}$ annihilations
$\overline{p}'s$ stop within the live data taking window [640-1650 ns]

- $\overline{p}'s$ are produced by the pW interactions in the PS.
- Very few $\overline{p}'s$ reach the DS, most of them stop within the first foil of the ST.
- $p\overline{p}$ annihilation at the ST can produce e^- by $\pi^0 \rightarrow \gamma\gamma$ decays followed by γ conversions and $\pi^- \rightarrow \mu^-\overline{\nu}$ decays followed by μ^- decays.
- $p\overline{p}$ annihilation in the TS can cause delayed Radiative Pion Capture.
- $\overline{p}'s$ cannot be efficiently suppressed by the time window cut used to reduce prompt background.

Antiproton background in Mu2e

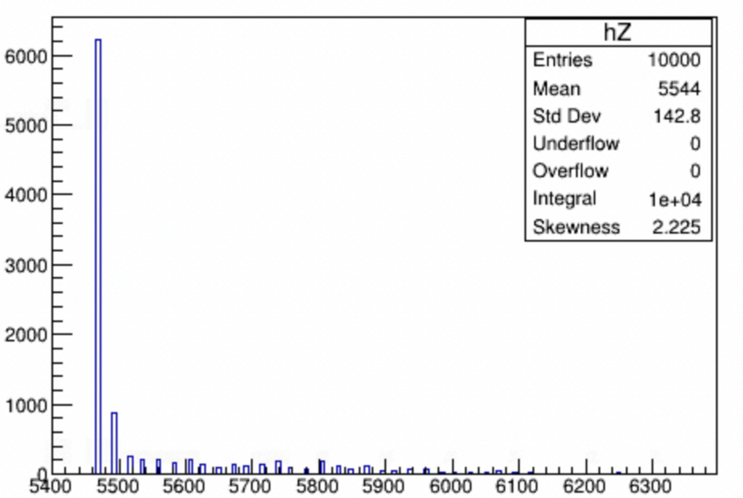

z (mm) from the centre of the TS
Longitudinal position of $\overline{p}$ annihilations

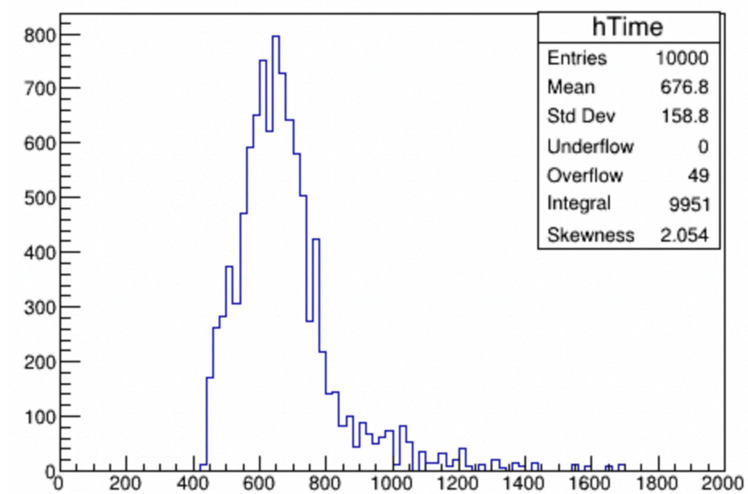

time (ns) of $\overline{p}$ annihilations
$\overline{p}'s$ stop within the live data taking window
[640-1650 ns]

- $\overline{p}'s$ are produced by the pW interactions in the PS.
- Very few $\overline{p}'s$ reach the DS, most of them stop within the first foil of the ST.
- $p\overline{p}$ annihilation at the ST can produce e^- by $\pi^0 \rightarrow \gamma\gamma$ decays followed by γ conversions and $\pi^- \rightarrow \mu^-\overline{\nu}$ decays followed by μ^- decays.
- $p\overline{p}$ annihilation in the TS can cause delayed Radiative Pion Capture.
- $\overline{p}'s$ cannot be efficiently suppressed by the time window cut used to reduce prompt background.
- Absorber elements placed at entrance and centre of the TS to suppress the $\overline{p}$ background.

Estimating the $\overline{p}$ background

Estimating the $\overline{p}$ background

- Background expected from $\overline{p}$ is low but highly uncertain.

Estimating the $\overline{p}$ background

- Background expected from $\overline{p}$ is low but highly uncertain.

- In 10^4 $p\overline{p}$ annihilation events, $\sim$ **20** events contain single e^- with $\geq$ 20 straw hits and momentum in the 90-110 MeV/c window.

Estimating the $\overline{p}$ background

- Background expected from $\overline{p}$ is low but highly uncertain.
- In 10^4 $p\overline{p}$ annihilation events, $\sim$ **20** events contain single e^- with $\geq$ 20 straw hits and momentum in the 90-110 MeV/c window.
- We can exploit another final state with much larger Branching Ratio and constrain the $\overline{p}$ background by comparison.

Estimating the $\overline{p}$ background

- Background expected from $\overline{p}$ is low but highly uncertain.

- In 10^4 $p\overline{p}$ annihilation events, $\sim$ **20** events contain single e^- with $\geq$ 20 straw hits and momentum in the 90-110 MeV/c window.

- We can exploit another final state with much larger Branching Ratio and constrain the $\overline{p}$ background by comparison.

- About 480 events contain $\geq$ **2 particles** with $\geq$ 20 straw hits per particle.

$$\frac{N_{e^- perMeV}}{N_{multi-track}} \approx \frac{1}{500}$$

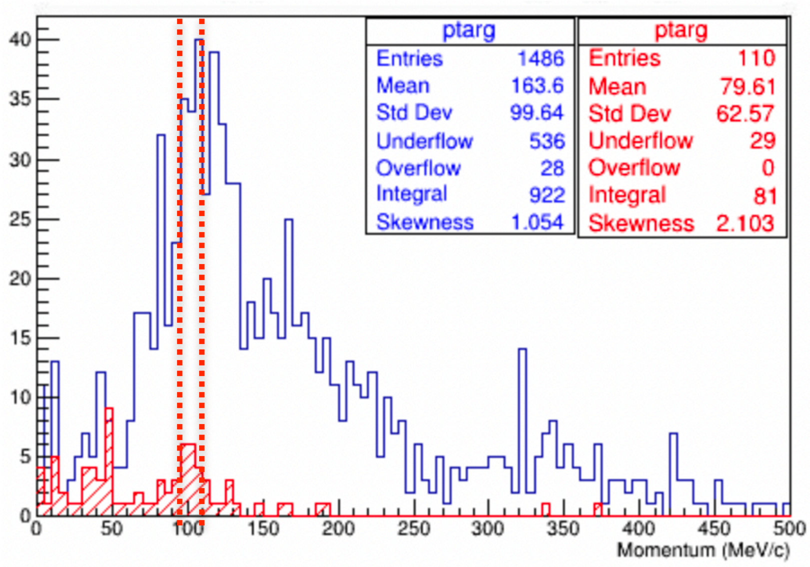

red: e^-

blue: multi-tracks

Total Momentum (MeV/c) after ST

Estimating the $\overline{p}$ background

- Background expected from $\overline{p}$ is low but highly uncertain.
- In 10^4 $p\overline{p}$ annihilation events, $\sim$ **20** events contain single e^- with $\geq$ 20 straw hits and momentum in the 90-110 MeV/c window.
- We can exploit another final state with much larger Branching Ratio and constrain the $\overline{p}$ background by comparison.
- About 480 events contain $\geq$ **2 particles** with $\geq$ 20 straw hits per particle.

$$\frac{N_{e^-perMeV}}{N_{multi-track}} \approx \frac{1}{500}$$

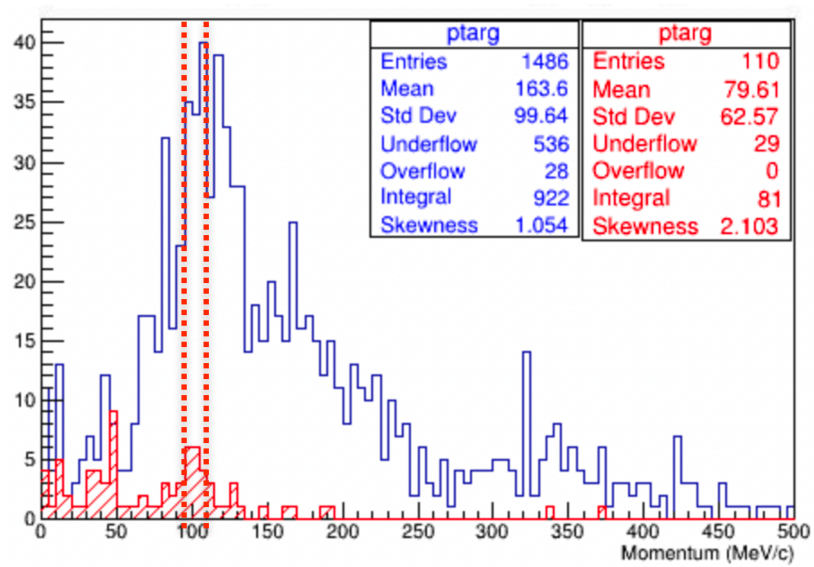

red: e^-
blue: multi-tracks

Total Momentum (MeV/c) after ST

Goal: Identify and reconstruct the multi-track final state events and get an estimate of the CE like events by rescaling the ratio of the two final states.

Single interaction $p\bar{p}$ annihilation events in the Mu2e detector

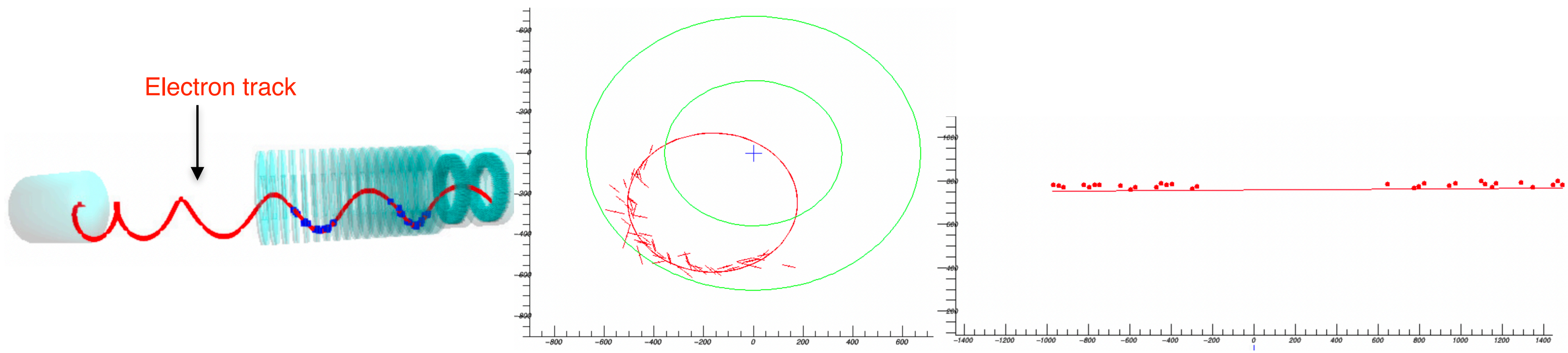

XY view | Time v/s z view

$p\bar{p}$ **annihilation in the ST events.** Red = electron, Green = Muon, Pink = Pion

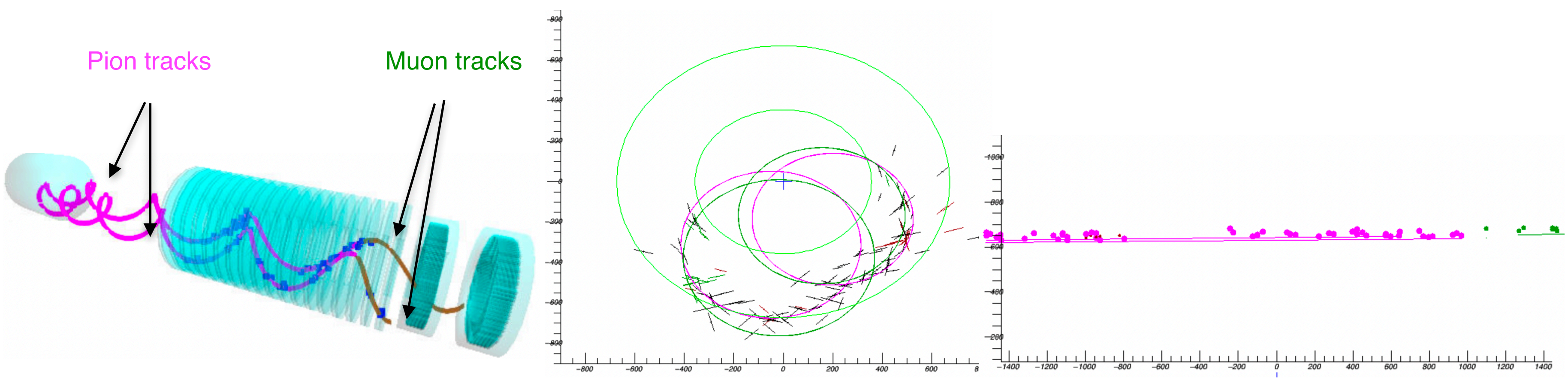

XY view | Time v/s z view

Goal: Identify and reconstruct the multi-track final state events and get an estimate of the CE like events by rescaling the ratio of the two final states.

Mu2e event reconstruction

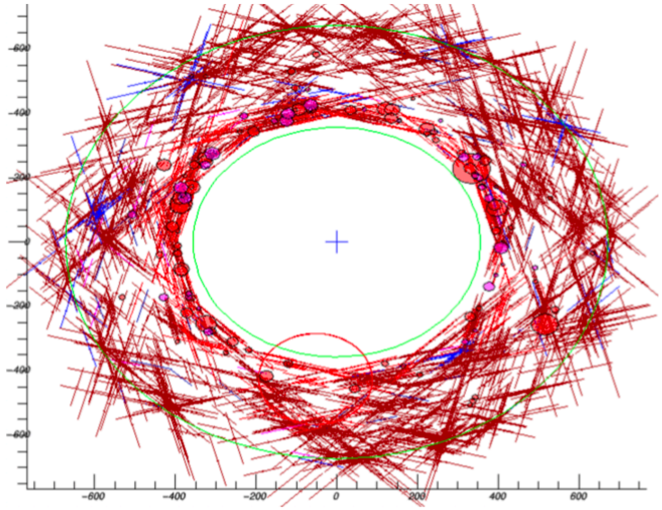

An event before background hits flagging
Blue: e+ Maroon: e-

Mu2e event reconstruction

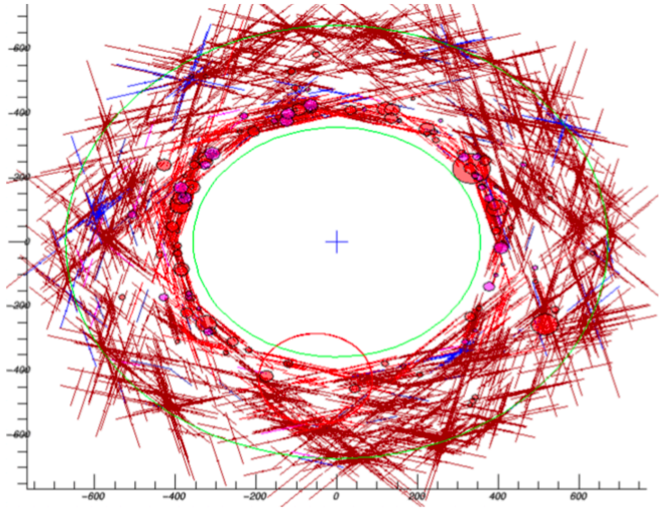

An event before background hits flagging
Blue: e+ Maroon: e-

- Mu2e event reconstruction is optimised for single-track events.

Mu2e event reconstruction

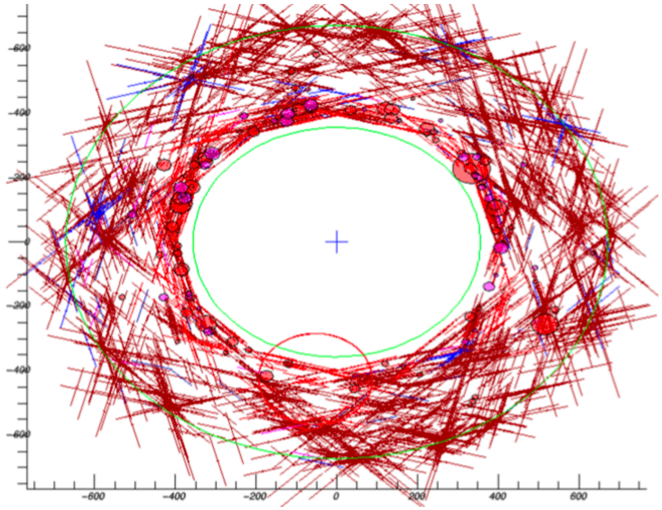

An event before background hits flagging
Blue: e+ Maroon: e-

- Mu2e event reconstruction is optimised for single-track events.
- From MC studies, > 90% of the hits in an event are from low energy e^+/e^- and protons. They are flagged as background.

Mu2e event reconstruction

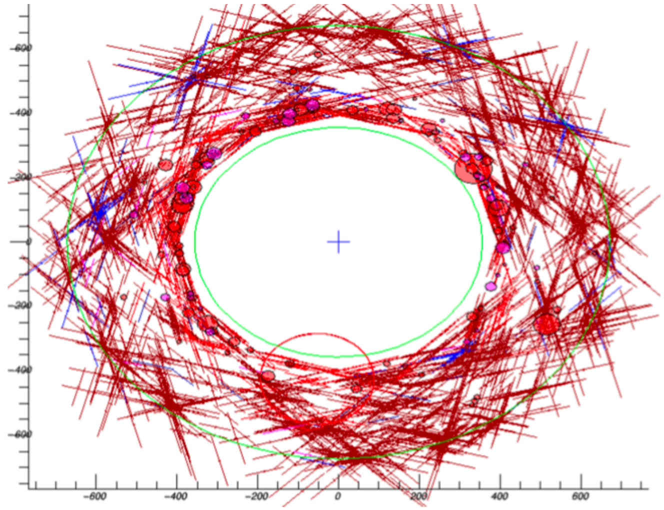

An event before background hits flagging

Blue: e+ Maroon: e-

- Mu2e event reconstruction is optimised for single-track events.
- From MC studies, > 90% of the hits in an event are from low energy e^+/e^- and protons. They are flagged as background.
- Assuming hits produced by the same particle have close reconstructed times, they are clustered in time.

Mu2e event reconstruction

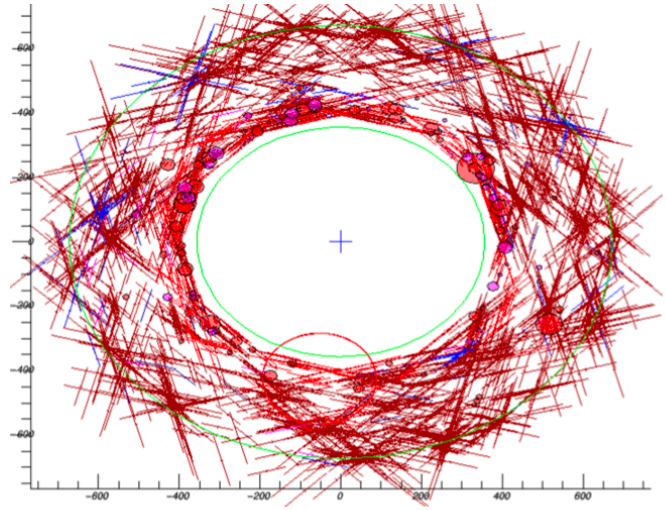

An event before background hits flagging
Blue: e+ Maroon: e-

- Mu2e event reconstruction is optimised for single-track events.
- From MC studies, > 90% of the hits in an event are from low energy e^+/e^- and protons. They are flagged as background.
- Assuming hits produced by the same particle have close reconstructed times, they are clustered in time.
- $TimeClusters$ are input for the pattern recognition which form the helical trajectories.

Mu2e event reconstruction

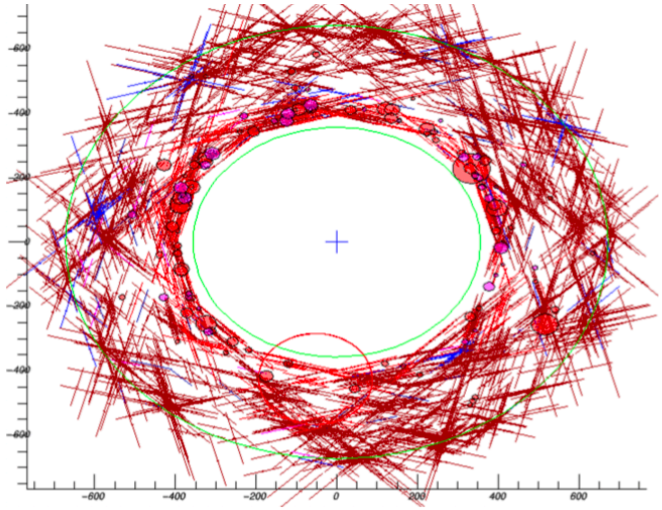

An event before background hits flagging
Blue: e+ Maroon: e-

- Mu2e event reconstruction is optimised for single-track events.
- From MC studies, > 90% of the hits in an event are from low energy e^+/e^- and protons. They are flagged as background.
- Assuming hits produced by the same particle have close reconstructed times, they are clustered in time.
- $TimeClusters$ are input for the pattern recognition which form the helical trajectories.
- Finally, parameters of the reconstructed track are determined by the Kalman fit.

Mu2e event reconstruction

* mu2e-docdb.fnal.gov/44935 ** mu2e-docdb.fnal.gov/43999

Mu2e event reconstruction

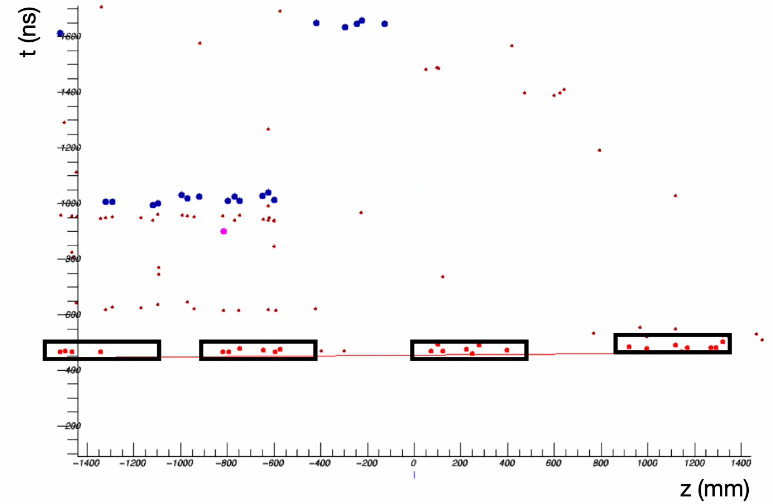

Time v/s z view of the hits in a CE + low intensity pileup event

* mu2e-docdb.fnal.gov/44935 ** mu2e-docdb.fnal.gov/43999

Mu2e event reconstruction

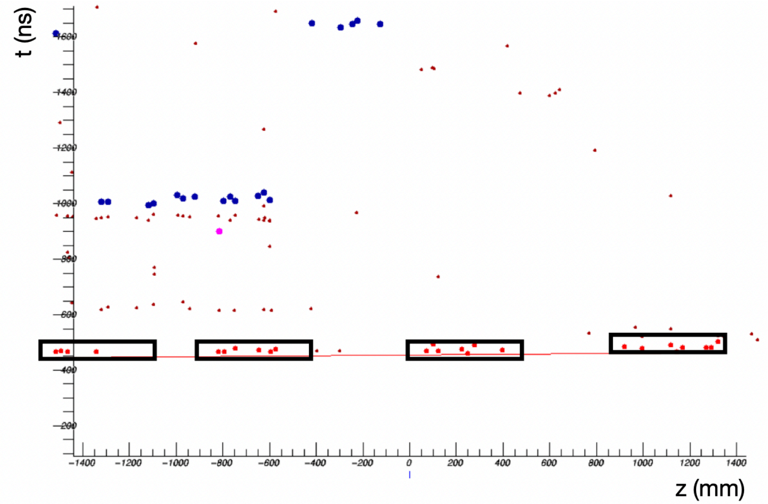

Time v/s z view of the hits in a CE + low intensity pileup event

- The default Mu2e algorithms removing the low energy hits and time clustering use an ANN which inadvertently remove a significant fraction of pion and muon hits.

* mu2e-docdb.fnal.gov/44935 ** mu2e-docdb.fnal.gov/43999

Mu2e event reconstruction

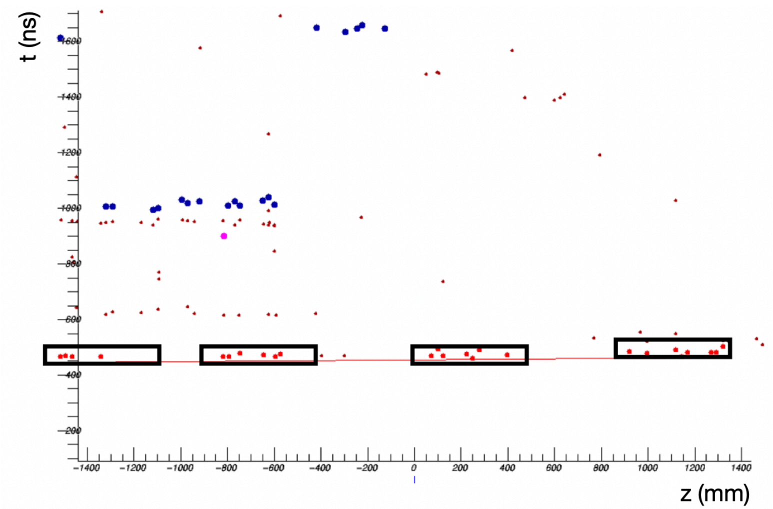

Time v/s z view of the hits in a CE + low intensity pileup event

- The default Mu2e algorithms removing the low energy hits and time clustering use an ANN which inadvertently remove a significant fraction of pion and muon hits.

- We have developed more physics-neutral algorithms, highly efficient for a wide spectrum of particle topologies to remove the low energy background hits* and time clustering**.

* mu2e-docdb.fnal.gov/44935 ** mu2e-docdb.fnal.gov/43999

Mu2e event reconstruction

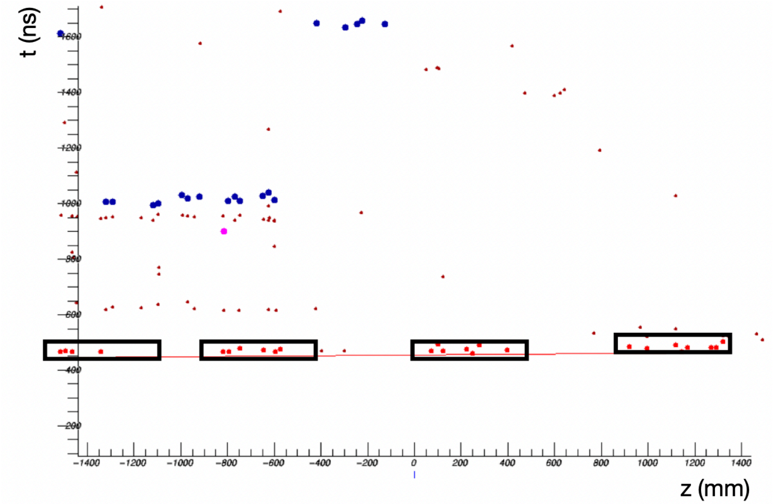

Time v/s z view of the hits in a CE + low intensity pileup event

- The default Mu2e algorithms removing the low energy hits and time clustering use an ANN which inadvertently remove a significant fraction of pion and muon hits.
- We have developed more physics-neutral algorithms, highly efficient for a wide spectrum of particle topologies to remove the low energy background hits* and time clustering**.
- The new time clustering algorithm searches for $TimeClusters$ using the hit time and z coordinates.

* mu2e-docdb.fnal.gov/44935 ** mu2e-docdb.fnal.gov/43999

Mu2e event reconstruction

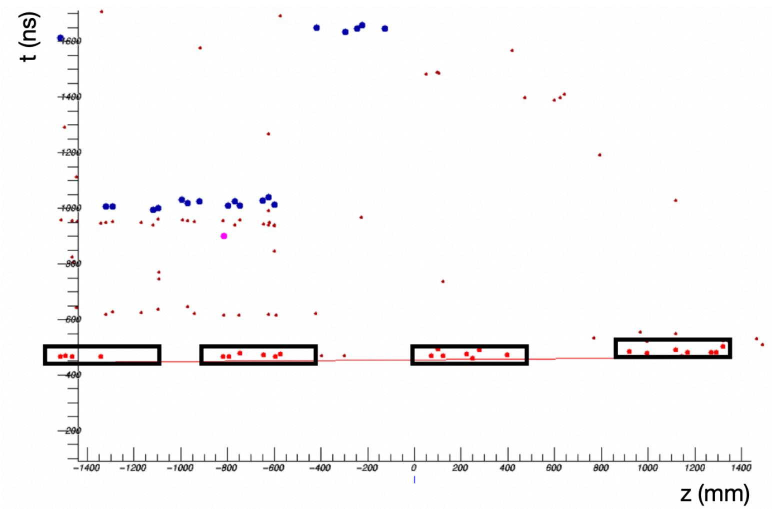

Time v/s z view of the hits in a CE + low intensity pileup event

- The default Mu2e algorithms removing the low energy hits and time clustering use an ANN which inadvertently remove a significant fraction of pion and muon hits.

- We have developed more physics-neutral algorithms, highly efficient for a wide spectrum of particle topologies to remove the low energy background hits* and time clustering**.

- The new time clustering algorithm searches for $TimeClusters$ using the hit time and z coordinates.

- With the new algorithms, the rejection factor of pions and muons have significantly reduced.

* mu2e-docdb.fnal.gov/44935 ** mu2e-docdb.fnal.gov/43999

Early Stage Hit Phi Clustering

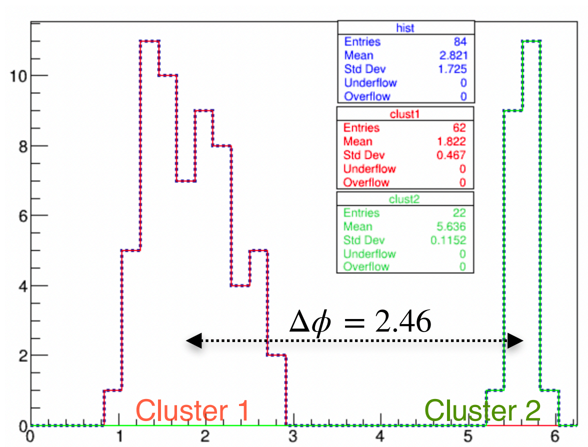

$\Delta\phi$ = 2.46 rad

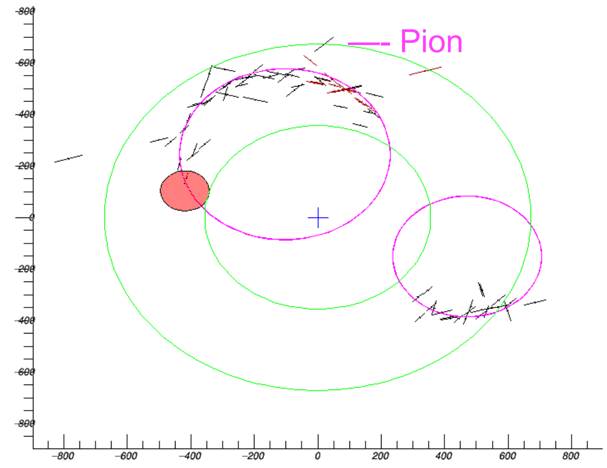

XY view

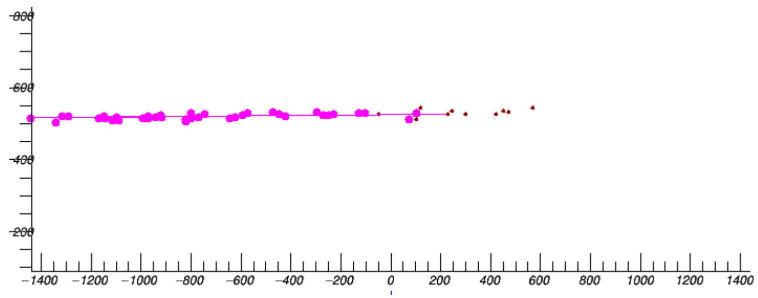

Time v/s z view

- Tracks from the same $p\overline{p}$ interaction could be close in time.
- Hits from different particles in the same time window could be well separated in ϕ or overlapping.
- We developed a ϕ clustering algorithm to group hits of a time cluster based on their ϕ distribution.

Comparing single interaction $p\bar{p}$ annihilation with CE events

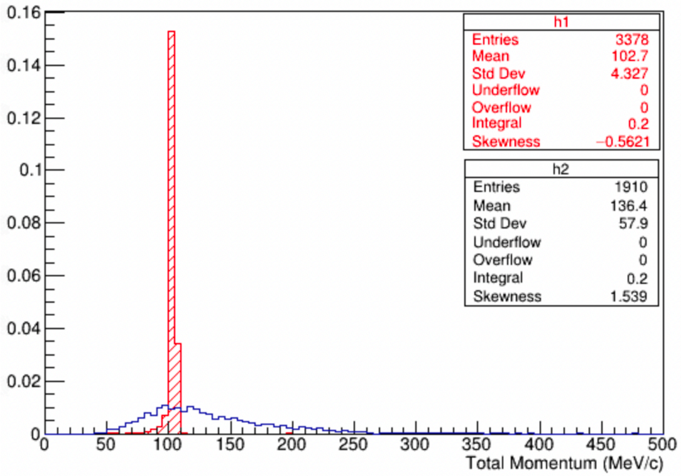

Total momentum

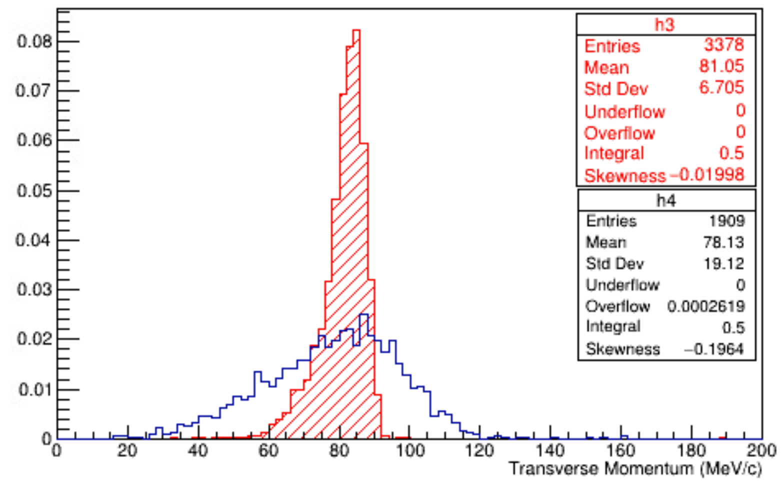

Transverse momentum

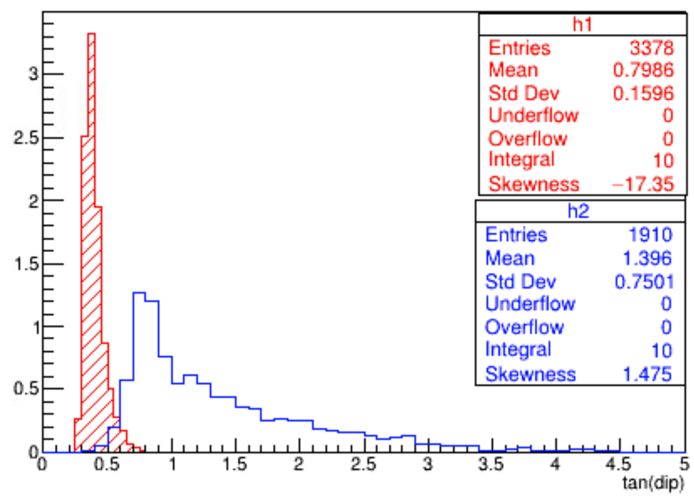

tan(λ)

— Conversion electron

— $p\bar{p}$ annihilation

- The topology of tracks from $p\bar{p}$ annihilation is much different from the expected CE tracks.
- $p\bar{p}$ annihilation tracks have a wider total momentum distribution and lower pitch than CE.

Preliminary results (single interaction $p\bar{p}$ annihilation events)

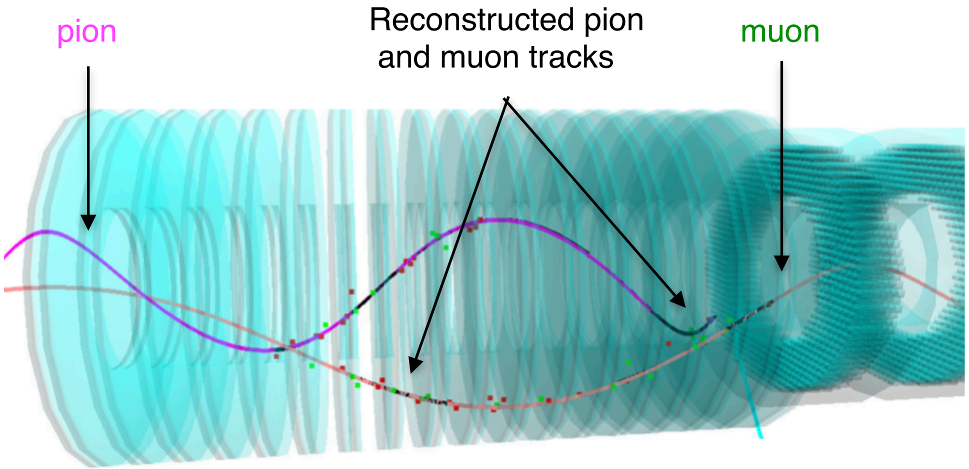

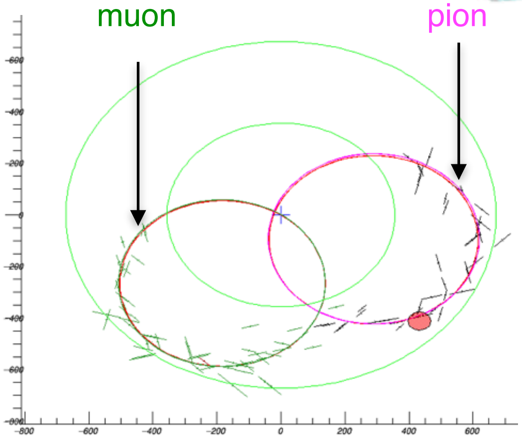

XY view

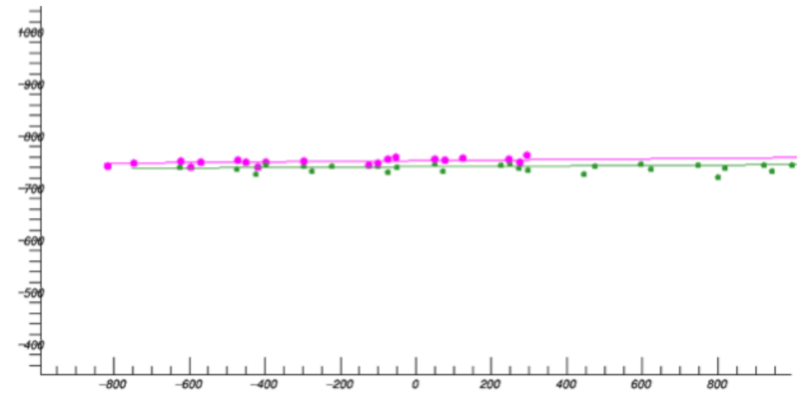

Time v/s z view

A $p\bar{p}$ annihilation at the ST event with two reconstructed tracks

Green = Muon, Pink = Pion, Black = Reconstructed track in 3-D view
Red = Reconstructed track in 2-D views

Comparison of default v/s new reconstruction with 10^4 single interaction $p\bar{p}$ annihilation events

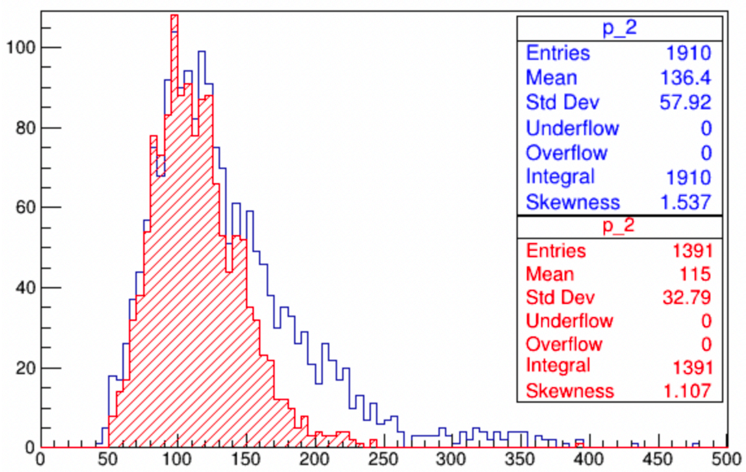

Total Momentum (MeV/c)

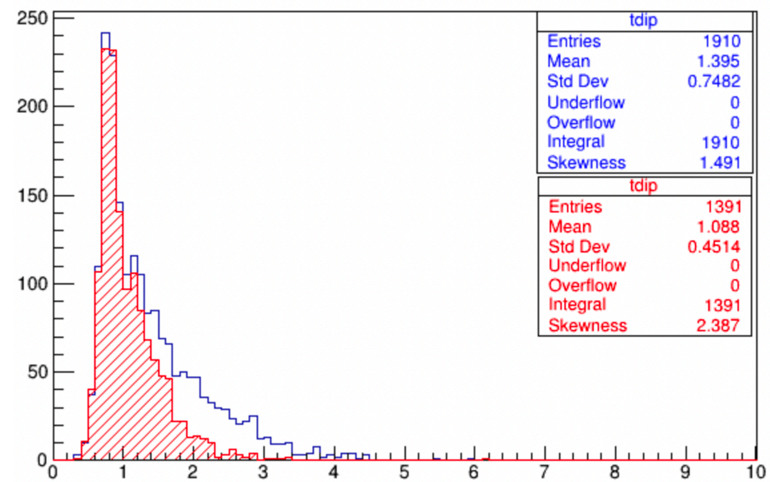

tan(λ)

- 18 events with single e^- track with $\geq$ 20 hits in the tracker, in the [90-110 MeV/c] momentum range were reconstructed.
- 137 multi-track events with each track having $\geq$ 20 hits in the tracker.

$$\left(\frac{N_{e^-perMeV}}{N_{multi-track}}\right)_{reco} \approx \frac{1}{140}$$

No. Of events with	>= 1 track	>= 2 tracks*
Default reco	1298	50
New reco	1709	109
Improvement factor	**x 1.3**	**x 2.2**

*Note: We have considered tracks with $\geq$ 20 hits in the tracker and momentum $\geq$ 80 MeV/c.

Preliminary results with $p\bar{p}$ annihilation + high intensity pile-up data sample

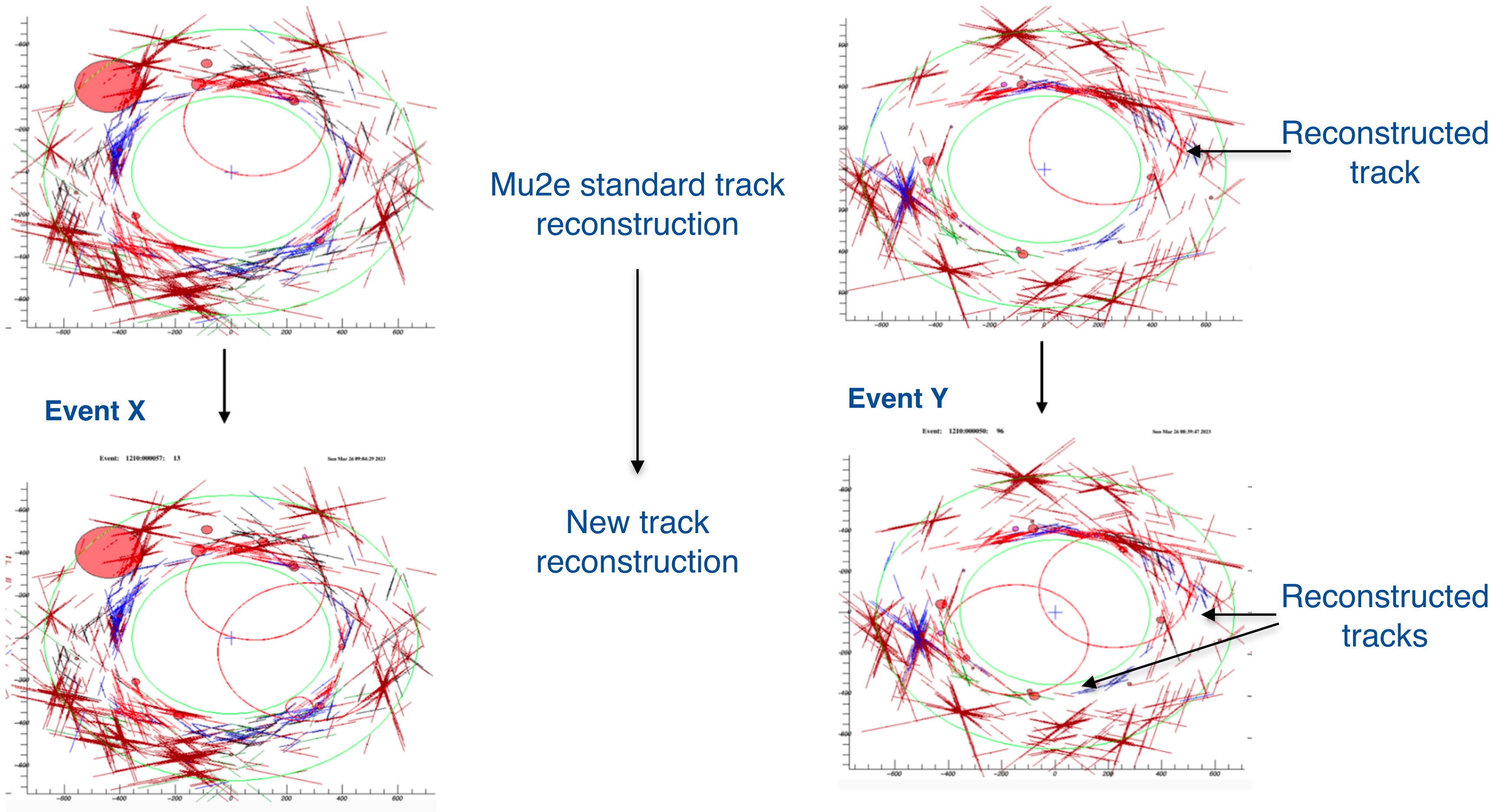

Transverse view of events from $p\bar{p}$ annihilation + high intensity pile-up data sample.
The red circle is the transverse view of the reconstructed track.
The segments are the "hit" tracker straws. The red circles are calorimeter clusters.

Default v/s new reconstruction with $p\bar{p}$ annihilation + pileup events

No. Of events with	>= 1 track	>= 2 tracks
Default reco	1089	46
New reco	1588	100
Improvement	**x 1.4**	**x 2.2**

1BB pileup

No. Of events with	>= 1 track	>= 2 tracks
Default reco	1046	39
New reco	1445	77
Improvement	**x 1.4**	**x 2**

2BB pileup

Default v/s new reconstruction with $p\bar{p}$ annihilation + pileup events

No. Of events with	>= 1 track	>= 2 tracks
Default reco	1089	46
New reco	1588	100
Improvement	**x 1.4**	**x 2.2**

1BB pileup

No. Of events with	>= 1 track	>= 2 tracks
Default reco	1046	39
New reco	1445	77
Improvement	**x 1.4**	**x 2**

2BB pileup

- Mu2e Run I will initially operate in the low intensity mode (1BB): mean intensity of 1.6×10^7 protons per pulse, ~ 25000 muons per pulse stop in the ST.

Default v/s new reconstruction with $p\bar{p}$ annihilation + pileup events

No. Of events with	>= 1 track	>= 2 tracks
Default reco	1089	46
New reco	1588	100
Improvement	**x 1.4**	**x 2.2**

1BB pileup

No. Of events with	>= 1 track	>= 2 tracks
Default reco	1046	39
New reco	1445	77
Improvement	**x 1.4**	**x 2**

2BB pileup

- Mu2e Run I will initially operate in the low intensity mode (1BB): mean intensity of 1.6×10^7 protons per pulse, ~ 25000 muons per pulse stop in the ST.
- We consider the reconstructed tracks with momentum ≥ 80 MeV/c making a minimum of 20 hits in the Tracker and with a $\chi^2/dof \leq 5$.

Default v/s **new** reconstruction with $p\bar{p}$ annihilation + pileup events

No. Of events with	>= 1 track	>= 2 tracks
Default reco	1089	46
New reco	1588	100
Improvement	**x 1.4**	**x 2.2**

1BB pileup

No. Of events with	>= 1 track	>= 2 tracks
Default reco	1046	39
New reco	1445	77
Improvement	**x 1.4**	**x 2**

2BB pileup

- Mu2e Run I will initially operate in the low intensity mode (1BB): mean intensity of 1.6×10^7 protons per pulse, ~ 25000 muons per pulse stop in the ST.
- We consider the reconstructed tracks with momentum ≥ 80 MeV/c making a minimum of 20 hits in the Tracker and with a $\chi^2/dof \leq 5$.
- We have several on-going efforts to improve the reconstruction efficiency further:

  -> A kinematic Kalman track fit (https://indico.jlab.org/459/papers/840-CHEP2023.pdf)
  -> Improved helix finder (https://indico.cern.ch/1252748/contributions/5521528/)
  -> ϕ-Z clean up of the $TimeClusters$ (mu2e-docdb.fnal.gov/docid=46832)

Contribution of DIO to multi-track events

Contribution of DIO to multi-track events

- For Run 1: $N_{ProtonsOnTarget} = 2.9 \times 10^{19},\ N_{\mu^{-}stops} = 4.6 \times 10^{16}$

Contribution of DIO to multi-track events

- For Run 1: $N_{ProtonsOnTarget} = 2.9 \times 10^{19}, \; N_{\mu^- stops} = 4.6 \times 10^{16}$

- 39% of stopped muons Decay in Orbit (DIO): $N_{DIO} = 4.6 \times 10^{16} \times 0.39 = 1.8 \times 10^{16}$

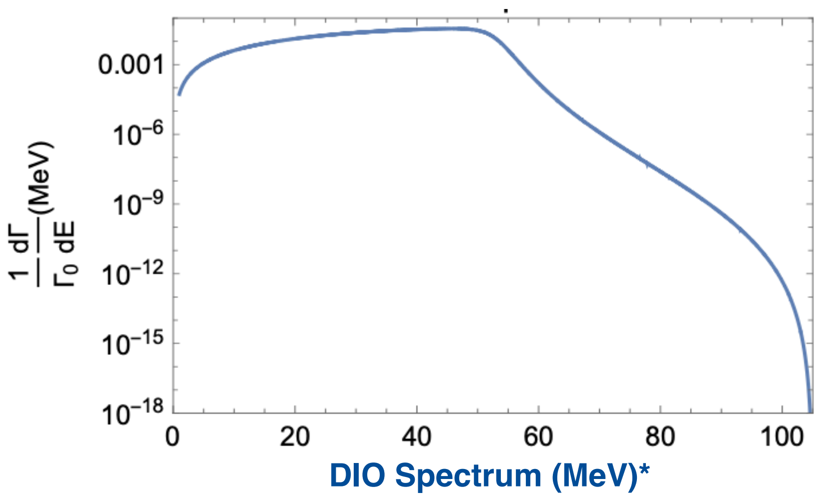

*Mu2e/Offline/heeckfinerbinning2016szafron.tbl

Contribution of DIO to multi-track events

- For Run 1: $N_{ProtonsOnTarget} = 2.9 \times 10^{19},\ N_{\mu^- stops} = 4.6 \times 10^{16}$

- 39% of stopped muons Decay in Orbit (DIO): $N_{DIO} = 4.6 \times 10^{16} \times 0.39 = 1.8 \times 10^{16}$

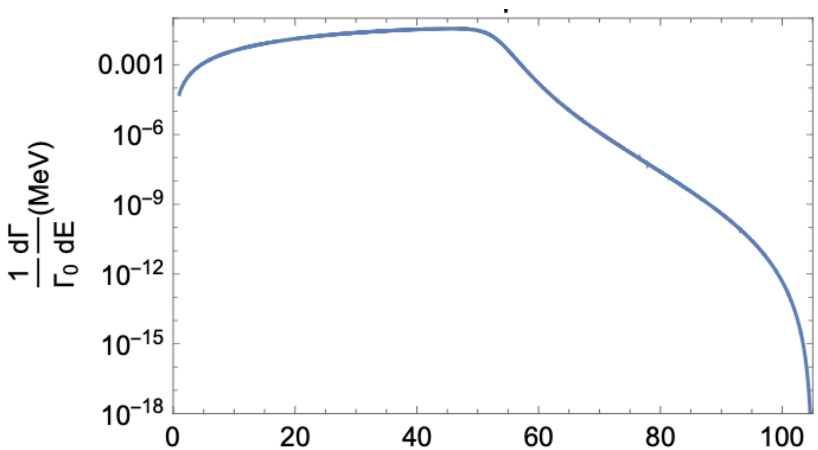

DIO Spectrum (MeV)*

- $N_{DIO>80MeV/c} = 1.8 \times 10^{16} \times 6.07 \times 10^{-8}$ $\qquad N_{2DIO>80MeV/c} = 66.24$

*Mu2e/Offline/heeckfinerbinning2016szafron.tbl

Contribution of DIO to multi-track events

- For Run 1: $N_{ProtonsOnTarget} = 2.9 \times 10^{19},\ N_{\mu^- stops} = 4.6 \times 10^{16}$

- 39% of stopped muons Decay in Orbit (DIO): $N_{DIO} = 4.6 \times 10^{16} \times 0.39 = 1.8 \times 10^{16}$

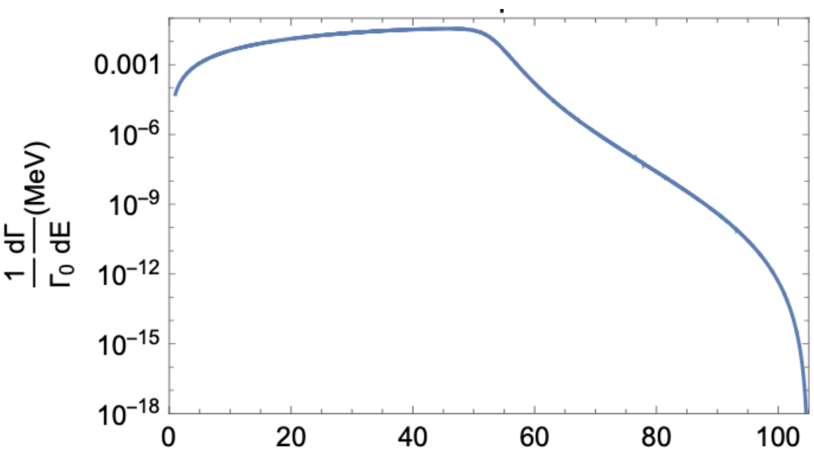

DIO Spectrum (MeV)*

- $N_{DIO>80MeV/c} = 1.8 \times 10^{16} \times 6.07 \times 10^{-8}$ $\quad N_{2DIO>80MeV/c} = 66.24$

- Assuming track reconstruction efficiency of $\sim$ 0.1,
  $N_{Reco2DIO>80MeV/c} \approx 0.66$ $\quad N_{Reco2DIO>85MeV/c} \approx 1.1 \times 10^{-4}$

*Mu2e/Offline/heeckfinerbinning2016szafron.tbl

Contribution of DIO to multi-track events

- For Run 1: $N_{ProtonsOnTarget} = 2.9 \times 10^{19}, \; N_{\mu^- stops} = 4.6 \times 10^{16}$

- 39% of stopped muons Decay in Orbit (DIO): $N_{DIO} = 4.6 \times 10^{16} \times 0.39 = 1.8 \times 10^{16}$

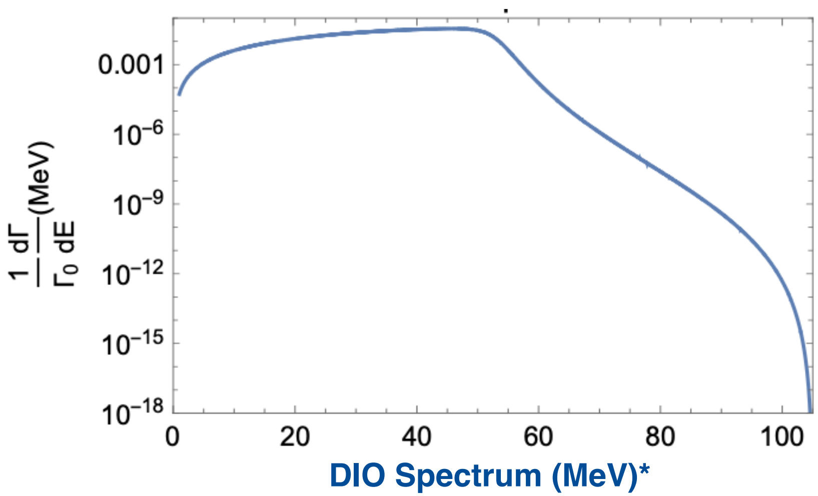

- $N_{DIO>80MeV/c} = 1.8 \times 10^{16} \times 6.07 \times 10^{-8}$ $\qquad N_{2DIO>80MeV/c} = 66.24$

- Assuming track reconstruction efficiency of ~ 0.1,
  $N_{Reco2DIO>80MeV/c} \approx 0.66$ $\qquad N_{Reco2DIO>85MeV/c} \approx 1.1 \times 10^{-4}$

- Assuming uniform DIO distribution in time and same efficiency of reconstruction for multi-track events as single-tracks:
  $N_{Reco2DIO>80MeV/c\Delta t<200ns} \approx 0.13$ $\qquad N_{Reco2DIO>85MeV/c\Delta t<200ns} \approx 2 \times 10^{-5}$

*Mu2e/Offline/heeckfinerbinning2016szafron.tbl

Contribution of cosmic muons to multi-track events

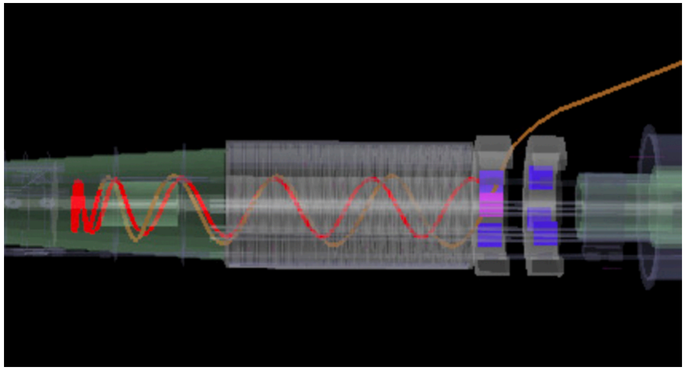

Event Y

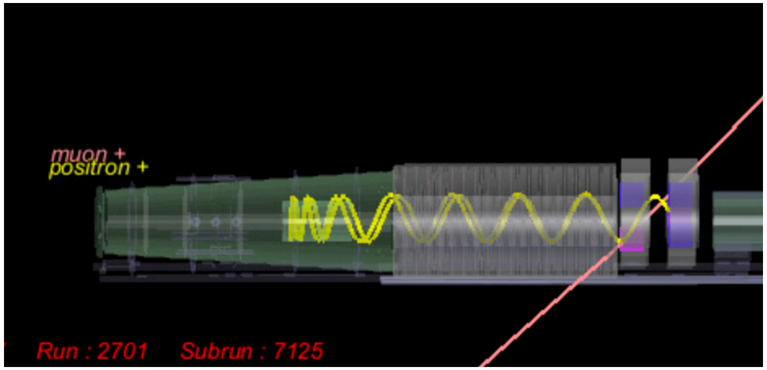

3-D view

Brown: μ^-, Pink: μ^+, Red: e^-, Yellow: e^+

* mu2e-docdb.fnal.gov/43526

Contribution of cosmic muons to multi-track events

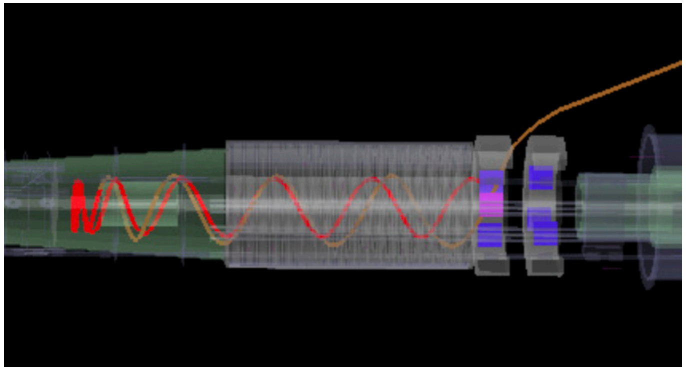

Event Y

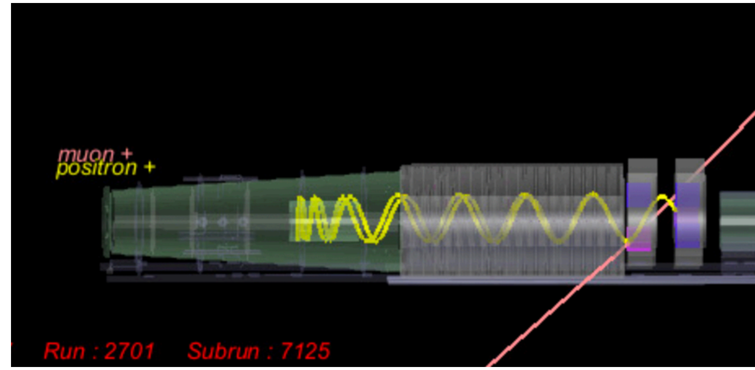

3-D view

Brown: μ^-, Pink: μ^+, Red: e^-, Yellow: e^+

- A Cosmic Ray Veto system composed of 4 layers of scintillator counters with embedded wavelength shifting fibres surrounds the DS.

* mu2e-docdb.fnal.gov/43526

Contribution of cosmic muons to multi-track events

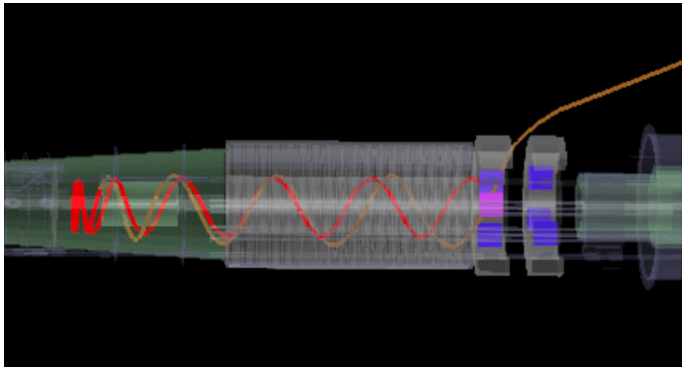

Event Y

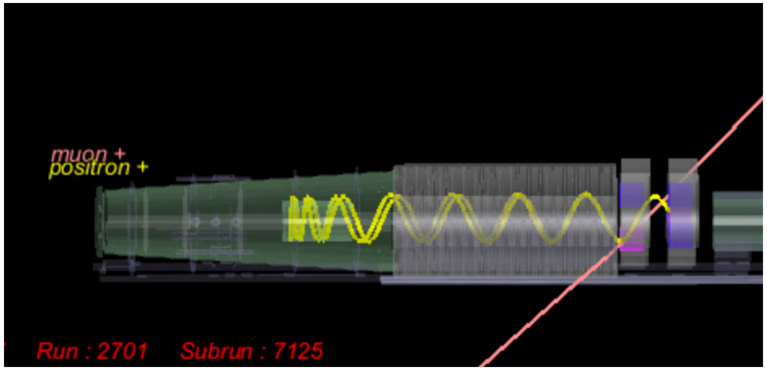

3-D view

Brown: μ^-, Pink: μ^+, Red: e^-, Yellow: e^+

- A Cosmic Ray Veto system composed of 4 layers of scintillator counters with embedded wavelength shifting fibres surrounds the DS.

- A track stub in at least 3/4 layers, localised in time and space produces a veto in offline analysis.

* mu2e-docdb.fnal.gov/43526

Contribution of cosmic muons to multi-track events

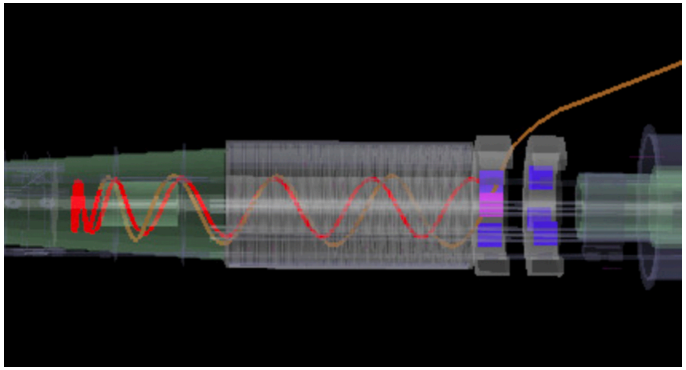

Event Y

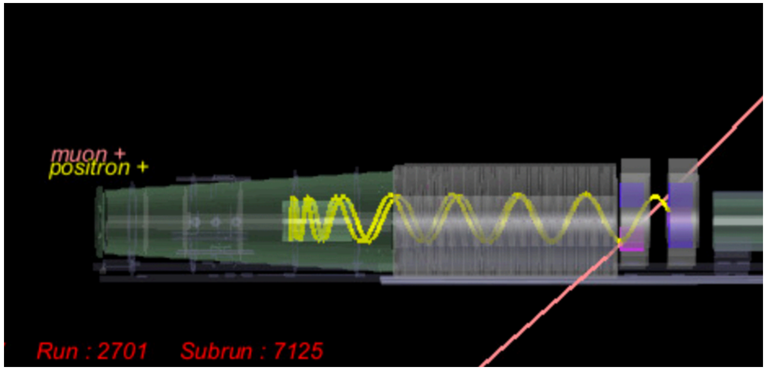

3-D view

Brown: μ^-, Pink: μ^+, Red: e^-, Yellow: e^+

- A Cosmic Ray Veto system composed of 4 layers of scintillator counters with embedded wavelength shifting fibres surrounds the DS.
- A track stub in at least 3/4 layers, localised in time and space produces a veto in offline analysis.
- The cosmic events were simulated using the CRY event generator*.

* mu2e-docdb.fnal.gov/43526

Contribution of cosmic muons to multi-track events

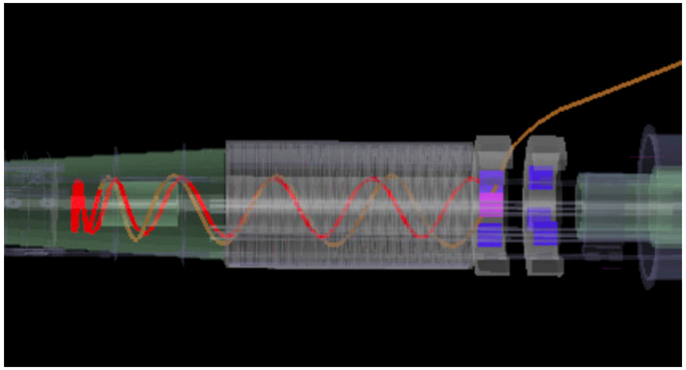

Event Y

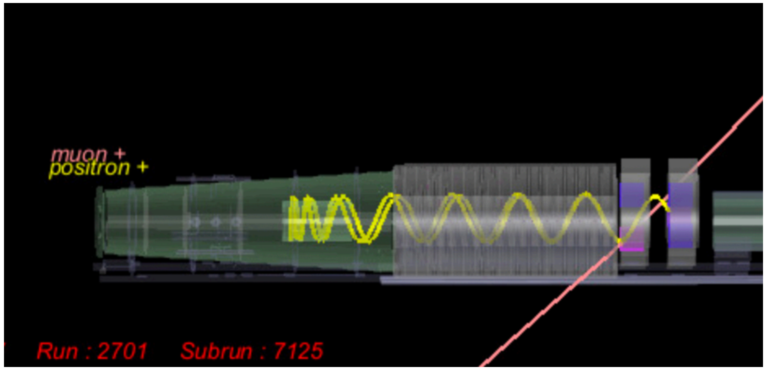

3-D view

Brown: μ^-, Pink: μ^+, Red: e^-, Yellow: e^+

- A Cosmic Ray Veto system composed of 4 layers of scintillator counters with embedded wavelength shifting fibres surrounds the DS.
- A track stub in at least 3/4 layers, localised in time and space produces a veto in offline analysis.
- The cosmic events were simulated using the CRY event generator*.
- We observed that the multi-track events from cosmics are usually:
  (1) Cosmic muons interacting with the calorimeter disk, producing an e^+/e^- which first travels upstream towards the ST and then returns back.
  (2) Cosmic muons interacting with the ST, producing e^+'s and e^-'s.

* mu2e-docdb.fnal.gov/43526

Contribution of cosmic muons to multi-track events

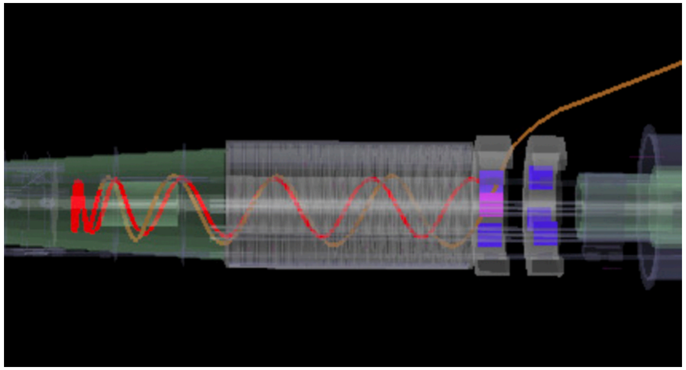

Event Y

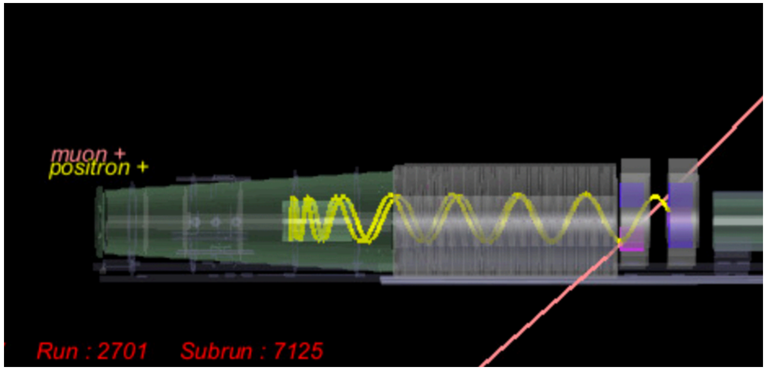

3-D view

Brown: μ^-, **Pink:** μ^+, **Red:** e^-, **Yellow:** e^+

- A Cosmic Ray Veto system composed of 4 layers of scintillator counters with embedded wavelength shifting fibres surrounds the DS.
- A track stub in at least 3/4 layers, localised in time and space produces a veto in offline analysis.
- The cosmic events were simulated using the CRY event generator*.
- We observed that the multi-track events from cosmics are usually:
  (1) Cosmic muons interacting with the calorimeter disk, producing an e^+/e^- which first travels upstream towards the ST and then returns back.
  (2) Cosmic muons interacting with the ST, producing e^+'s and e^-'s.
- While $p\bar{p}$ annihilation at the ST mostly produces pions and muons.

* mu2e-docdb.fnal.gov/43526

Summary

Summary

- We are developing a novel data-driven approach to constrain the antiproton background in Mu2e.

Summary

- We are developing a novel data-driven approach to constrain the antiproton background in Mu2e.
- The Mu2e detector and the default event reconstruction procedure are designed for efficient reconstruction of single track events. The topology of a multi-track $p\bar{p}$ annihilation event is very different from a CE event.

Summary

- We are developing a novel data-driven approach to constrain the antiproton background in Mu2e.
- The Mu2e detector and the default event reconstruction procedure are designed for efficient reconstruction of single track events. The topology of a multi-track $p\bar{p}$ annihilation event is very different from a CE event.
- Using the new reconstruction sequence number of events with ≥ 2 tracks increased by $\sim \times 2.1$ for the $p\bar{p}$ annihilation events.

Summary

- We are developing a novel data-driven approach to constrain the antiproton background in Mu2e.

- The Mu2e detector and the default event reconstruction procedure are designed for efficient reconstruction of single track events. The topology of a multi-track $p\overline{p}$ annihilation event is very different from a CE event.

- Using the new reconstruction sequence number of events with ≥ 2 tracks increased by $\sim \times 2.1$ for the $p\bar{p}$ annihilation events.

- The new algorithms not only significantly improve the efficiency of reconstructing $p\overline{p}$ annihilation events, but they also improve the efficiency of single e^- track reconstruction.

Summary

- We are developing a novel data-driven approach to constrain the antiproton background in Mu2e.

- The Mu2e detector and the default event reconstruction procedure are designed for efficient reconstruction of single track events. The topology of a multi-track $p\bar{p}$ annihilation event is very different from a CE event.

- Using the new reconstruction sequence number of events with ≥ 2 tracks increased by $\sim \times 2.1$ for the $p\bar{p}$ annihilation events.

- The new algorithms not only significantly improve the efficiency of reconstructing $p\bar{p}$ annihilation events, but they also improve the efficiency of single e^- track reconstruction.

- If we consider each track to have $p \geq 85$ MeV/c, then the number of two-track events from DIO for Run 1 is estimated to be $\sim 2 \times 10^{-5}$ events.

Summary

- We are developing a novel data-driven approach to constrain the antiproton background in Mu2e.
- The Mu2e detector and the default event reconstruction procedure are designed for efficient reconstruction of single track events. The topology of a multi-track $p\bar{p}$ annihilation event is very different from a CE event.
- Using the new reconstruction sequence number of events with ≥ 2 tracks increased by $\sim \times 2.1$ for the $p\bar{p}$ annihilation events.
- The new algorithms not only significantly improve the efficiency of reconstructing $p\bar{p}$ annihilation events, but they also improve the efficiency of single e^- track reconstruction.
- If we consider each track to have $p \geq 85$ MeV/c, then the number of two-track events from DIO for Run 1 is estimated to be $\sim 2 \times 10^{-5}$ events.

Summary

- We are developing a novel data-driven approach to constrain the antiproton background in Mu2e.
- The Mu2e detector and the default event reconstruction procedure are designed for efficient reconstruction of single track events. The topology of a multi-track $p\bar{p}$ annihilation event is very different from a CE event.
- Using the new reconstruction sequence number of events with ≥ 2 tracks increased by $\sim \times 2.1$ for the $p\bar{p}$ annihilation events.
- The new algorithms not only significantly improve the efficiency of reconstructing $p\bar{p}$ annihilation events, but they also improve the efficiency of single e^- track reconstruction.
- If we consider each track to have $p \geq 85$ MeV/c, then the number of two-track events from DIO for Run 1 is estimated to be $\sim 2 \times 10^{-5}$ events.
- We have obtained $\left(\frac{N_{e^- perMeV}}{N_{multi-track}}\right)_{reco} \approx \frac{1}{140}$ for single interaction $p\bar{p}$ annihilation events in Mu2e. We plan to improve this ratio further.

This work was supported by the EU Horizon 2020 Research and Innovation Program under the Marie Sklodowska-Curie Grant Agreement Nos. 734303, 822185, 858199, 101003460.

Extra slides

Charged Lepton Flavour Violation (CLFV)

- According to the Standard Model (SM), lepton flavour is always conserved in all interactions.
- The discovery of neutrino oscillations prove that interactions of the SM leptons are non-diagonal in flavour.
- But, the branching fractions of CLFV processes through neutrino oscillations are suppressed by factors proportional to $(\Delta m_\nu^2)^2/M_W^4$ to **undetectably tiny** levels, $< 10^{-50}$.
- Many New Physics models predict much higher rates of CLFV.

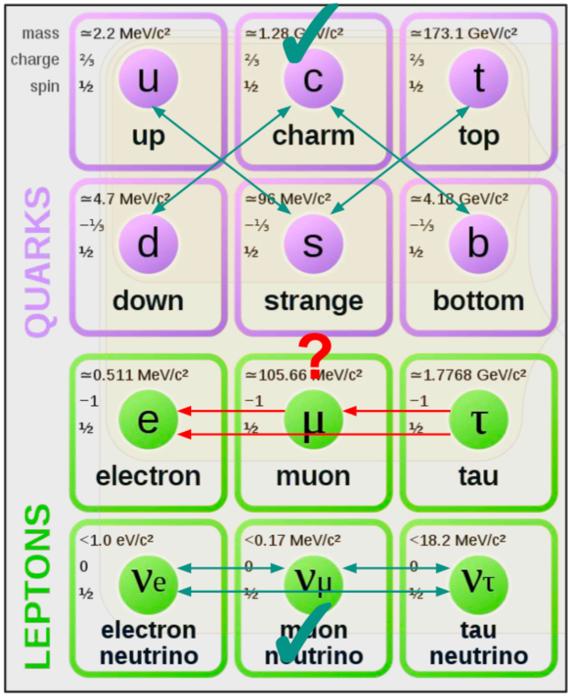

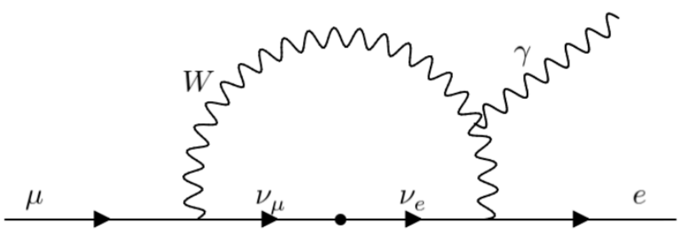

Observation of a CLFV process would be unambiguous evidence of New Physics

Search for CLFV

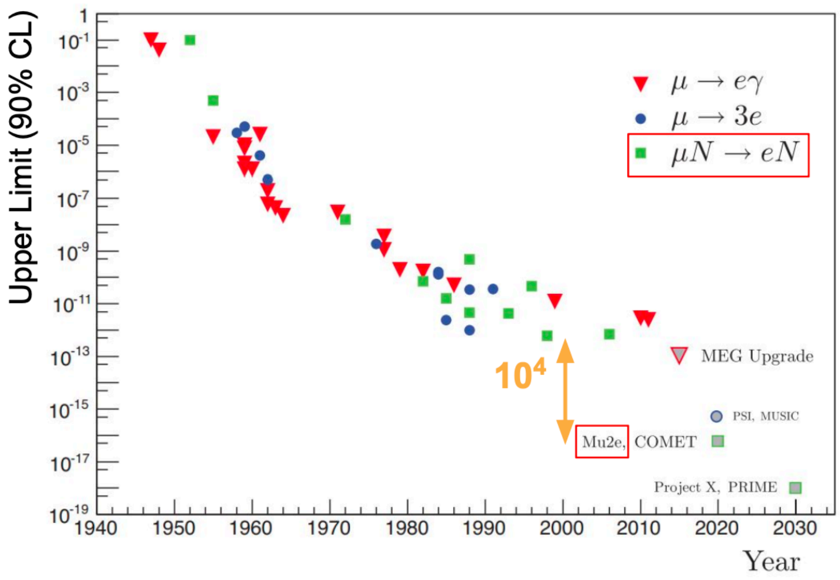

Experiments looking for CLFV: Past, Present and Future

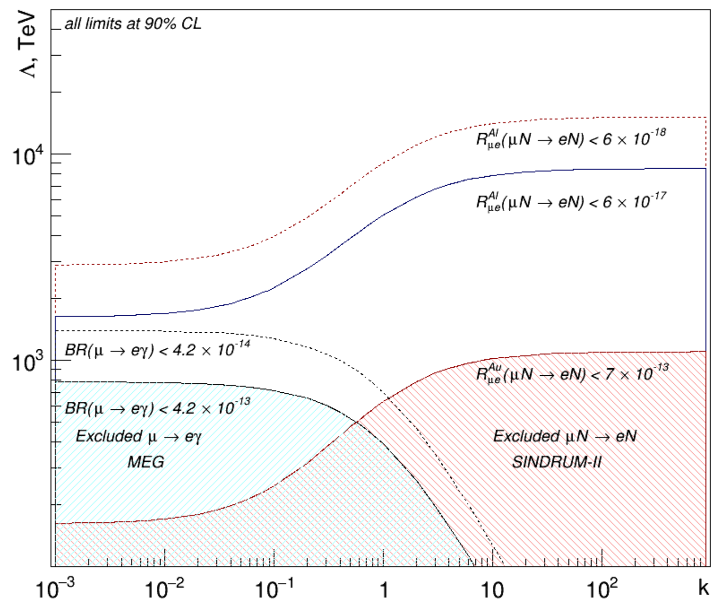

Λ is the effective mass scale and κ controls the relative contribution of the dipole moment term and the four fermion term

$$\mathscr{L}_{CLFV} = \frac{m_\mu}{(1+\kappa)\Lambda^2}\bar{\mu}_R\sigma_{\mu\nu}e_L F^{\mu\nu} + \frac{\kappa}{1+\kappa}\bar{\mu}_L\gamma_\mu e_L \sum_{q=u,d} \overline{q_L}\gamma^\mu q_L$$

- The $\mu^- N \to e^- N$ conversion channel:
  -> No combinatorial background.
  -> Best sensitivity to CLFV in a large range of NP scenarios.
  -> Can give unique information regarding underlying NP operators.

- Current best limit on $\mu^- N \to e^- N$ set by SINDRUM II experiment: $R_{\mu e} < 7 \times 10^{-13}$ (90% C.L).

*Andr´e de Gouv^ea Petr Vogel

CLFV with Muons: EFT Picture

Loop term | Contact term

$$\mathcal{L}_{\mathrm{CLFV}} = \frac{m_\mu}{(1+\kappa)\Lambda^2}\bar{\mu}_R\sigma_{\mu\nu}e_L F^{\mu\nu} + \frac{\kappa}{(1+\kappa)\Lambda^2}\bar{\mu}_L\gamma_\mu e_L\left(\sum_{q=u,d}\bar{q}_L\gamma^\mu q_L\right)$$

- Parameterize with dimension six EFT terms added to the SM Lagrangian ($\propto 1/\Lambda^2$)
  - Loop term: e.g. SUSY, heavy ν's ...
  - Contact term: e.g. leptoquarks, heavy Z …
- **Mu2e sensitive to both types of terms***
- Λ mass scale -- **Mu2e will probe $\Lambda \sim 10^4$ TeV**
- κ tunes relative contribution from each term

- Note that other EFT parameterizations exist
  [e.g. Davidson and Echenard DOI:10.1140/epjc/s10052-022-10773-4]

Loop term

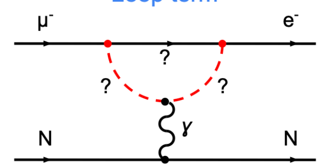

Contact term

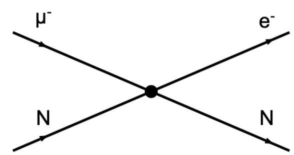

* There are 4 lepton contact operators that Mu2e is sensitive to at loop level, and Mu3e is sensitive to at leading order.

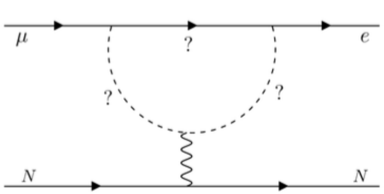

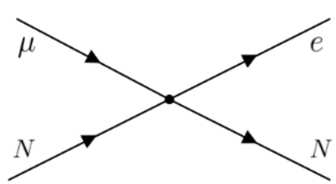

Science Motivation

- Direct μ→e conversion is the "Golden Channel" of CLFV
  – Sensitive to broad array of New Physics models

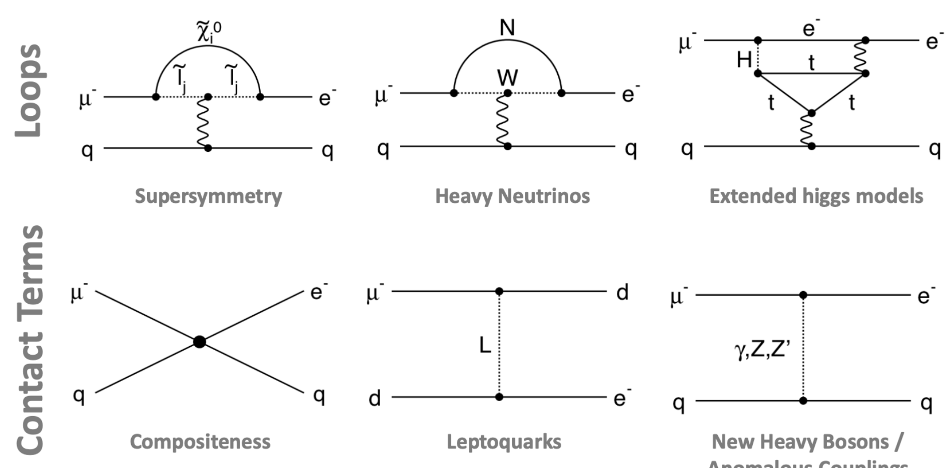

e.g.: $Br(\mu \to e\gamma) = \frac{3\alpha}{32\pi}\left|\sum_{i=2,3} U^*_{\mu i} U_{ei} \frac{\Delta m^2_{1i}}{M^2_W}\right|^2 < 10^{-54}$

[$U_{\alpha i}$ are the elements of the leptonic mixing matrix,
$\Delta m^2_{1i} \equiv m^2_i - m^2_1$, $i = 2, 3$ are the neutrino mass-squared differences]

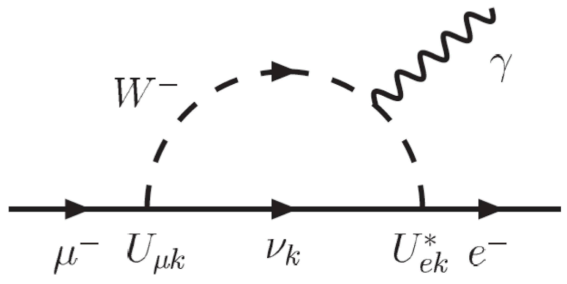

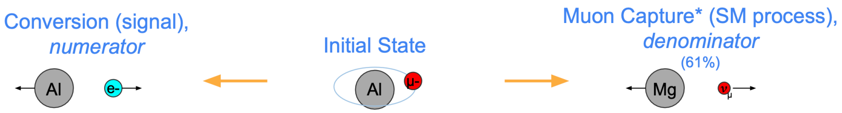

What does "Λ" mean?

This is clearly model dependent! However, some general issues are easy to identify…

- $\mu \to e\gamma$ always occurs at the loop level, and is suppressed by the E&M coupling e. Also chiral suppression (potential for "$\tan\beta$" enhancement).

$$\frac{1}{\Lambda^2} \sim \frac{e}{16\pi^2}\frac{\tan\beta}{M^2_{\rm new}}$$

- $\mu \to eee$ and $\mu \to e$-conversion in nuclei can happen at the tree-level

$$\frac{1}{\Lambda^2} \sim \frac{y^2_{\rm new}}{M^2_{\rm new}}$$

Science Motivation

- Direct $\mu \rightarrow e$ conversion is the "Golden Channel" of CLFV
  - Once an observation is made, can change stopping target to probe underlying NP operator
  - However Mu2e-II would be limited by muonic atom lifetimes to nuclei below Z~40 due to delayed time window for acceptable events. Examples of muonic atom lifetimes:

  Al (864 ns), Ti((330 ns), V(285 ns), Pb(74.8 ns)

	S	D	V^1	V^2
$\frac{B(\mu \to e, \mathrm{Ti})}{B(\mu \to e, \mathrm{Al})}$	$1.70 \pm 0.005_y$	1.55	1.65	2.0
$\frac{B(\mu \to e, \mathrm{Pb})}{B(\mu \to e, \mathrm{Al})}$	$0.69 \pm 0.02_{\rho_n}$	1.04	1.41	$2.67 \pm 0.06_{\rho_n}$

y = nuclear scalar form factor, ρ_n = nuclear neutron density

V. Cirigliano et al., phys. Rev. **D80** 013002 (2009)

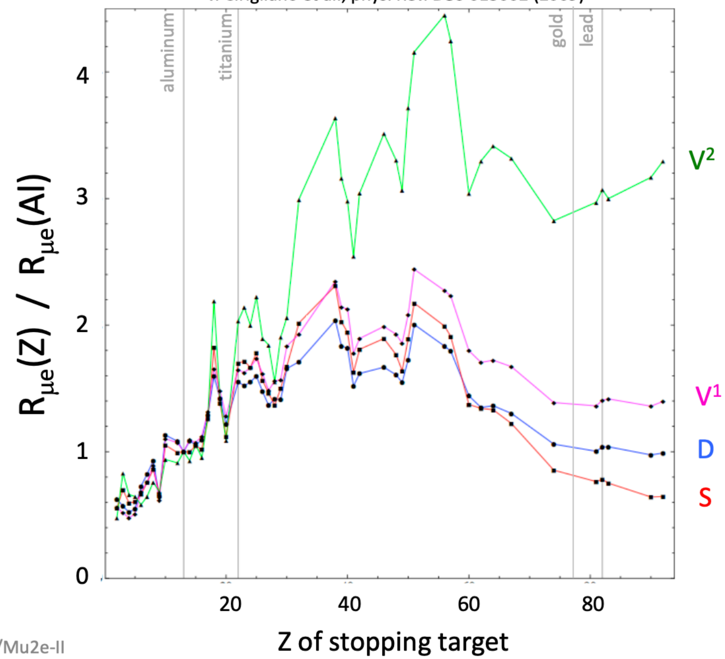

charged-lepton flavor violation were to be experimentally detected, it would have to come from "new physics" such as supersymmetry, heavy neutrino mixing, leptoquark interactions, or some other extension of the standard model. In that way, charged-lepton number violating reactions provide a discovery window to interactions, beyond standard model expectations, reaching effective-mass scales above $\mathcal{O}(1000\ \mathrm{TeV})$ [1,2].

Because muons can be copiously produced at accelerators and are relatively long lived (2.2 μs), they have been at the forefront of searches for CLFV [1,2]. One reaction that can be probed with particularly high sensitivity is the muon-electron conversion in a muonic atom,

$$\mu^- + (A, Z) \rightarrow e^- + (A, Z), \qquad (1)$$

where (A, Z) represents a nucleus of atomic number Z and mass number A. Various experiments have been performed over the years to search for this process [3]. The most

MEG experiment [10]. In addition, the conversion process is also sensitive to CLFV chiral conserving amplitudes that do not contribute to $\mu \rightarrow e\gamma$.

The success of the conversion searches depends critically on control of the background events. The signal for the $\mu - e$ conversion process in Eq. (1) is a monoenergetic electron with energy $E_{\mu e}$, given by

$$E_{\mu e} = m_\mu - E_b - E_{\mathrm{rec}}, \qquad (2)$$

where m_μ is the muon mass, $E_b \simeq Z^2\alpha^2 m_\mu/2$ is the binding energy of the muonic atom, and $E_{\mathrm{rec}} \simeq m_\mu^2/(2m_N)$ is the nuclear-recoil energy, with α the fine-structure constant, and m_N the nucleus mass. The main physics background for this signal comes from the so-called muon decay-in-orbit (DIO), a process in which the muon decays in the normal way, i.e. $\mu^- \rightarrow e^- \bar{\nu}_e \nu_\mu$, while in the orbit of the atom. Whereas in a free-muon decay, in order to

Background processes to $\mu^- \to e^-$ search

- Decay in Orbit : In free μ^-decay, e^- kinematic endpoint is $m_\mu/2$. In the field of a nucleus, μ^- decay endpoint is extended to the signal energy.

- Radiative Pion Capture: $\pi^- + N(A,Z) \to \gamma(e^+e^-) + N(A,Z-1)$
  Due to the short lifetime of pions, this background can be suppressed by using pulsed p beam with a delayed live-time window.

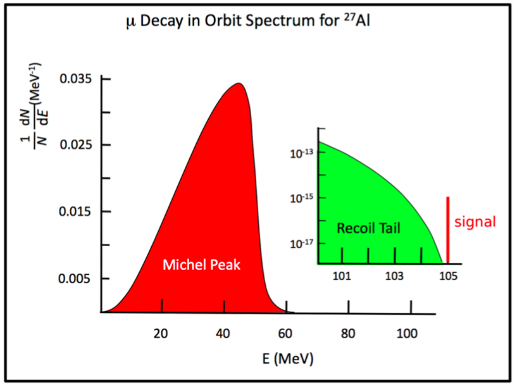

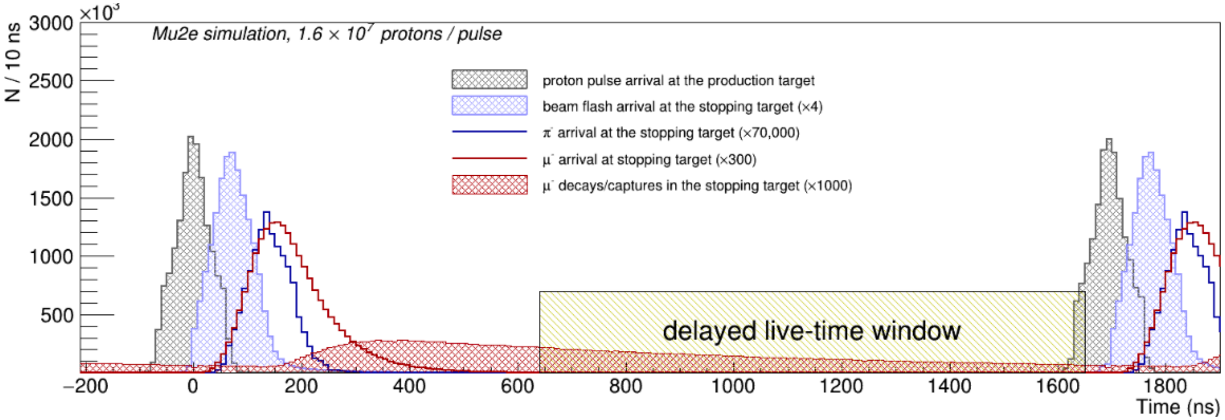

- Cosmic Rays: interacting or decaying within the detector are expected to produce ~1 signal like event per day. The cosmic ray veto system surrounds the DS to detect the cosmic rays.

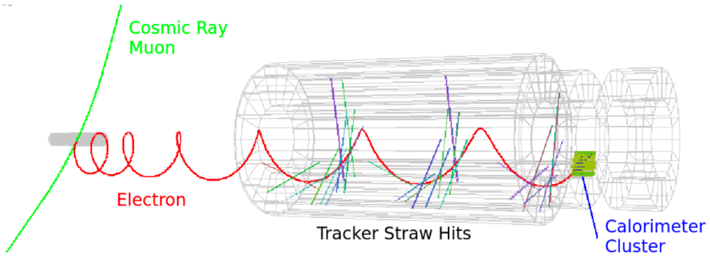

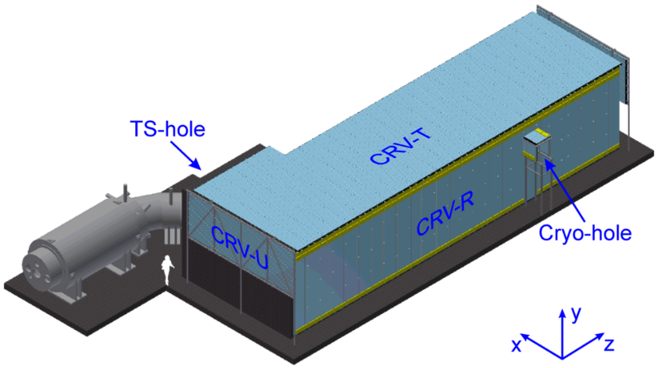

Main Mu2e Detectors

- Straw tube tracker

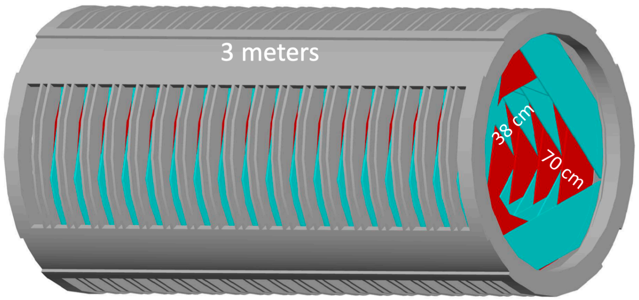

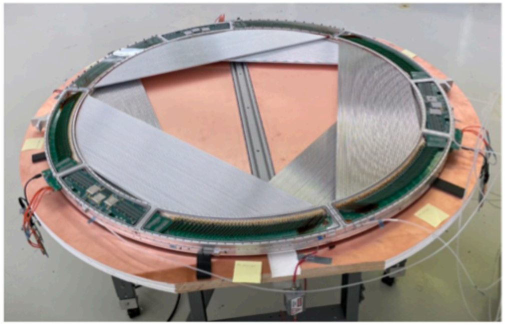
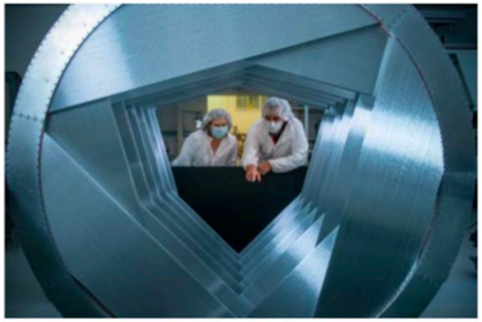

18 stations, 2 planes per station, 12 panels per plane, 96 straws per panel.
Straws filled with 80%:20% $Ar : CO_2$ mixture.
For 100 MeV/c electrons, the intrinsic momentum resolution of the tracker is $\Delta p_{trk} < 300$ keV/c FWHM.

- Electromagnetic Calorimeter

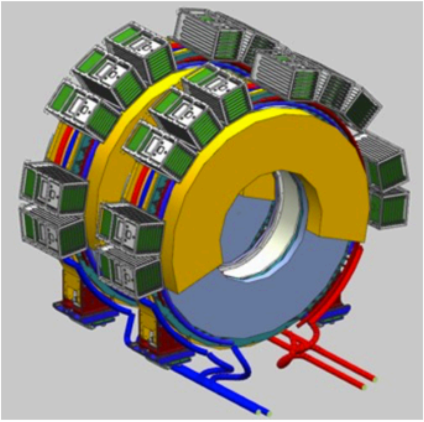
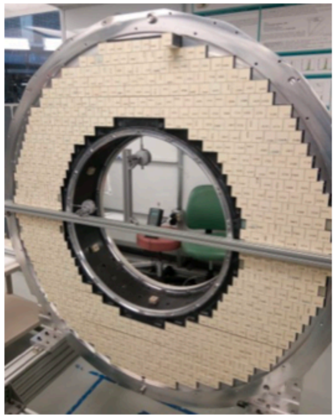

2 disks covering radii 37 cm - 66 cm. Each disk has 674 pure CsI crystals.
Test beam results for 100 MeV e- beam give energy resolution of 16.4% FWHM and timing resolution of 110 ps*.

*Atanova et al *Journal of Instrumentation* **2017**

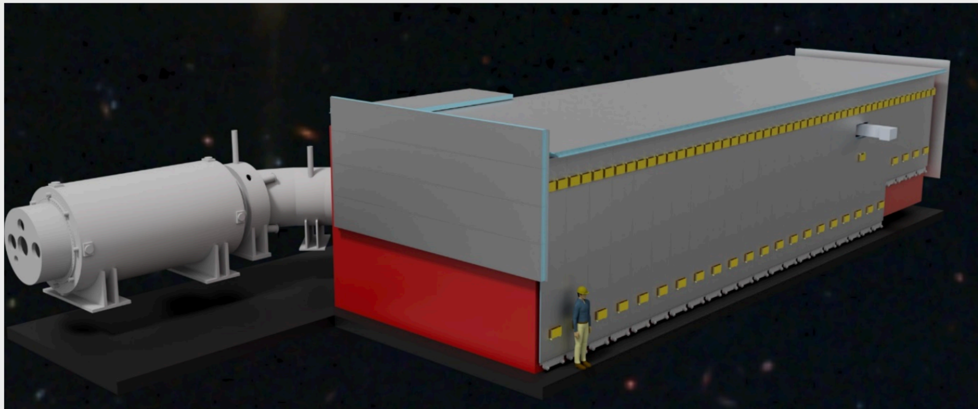

Details:

- Area: 335 m²
- 83 modules; 10 types
- 5,376 counters
- 10,752 fibers
- 19,456 SiPMs
- 4,864 Counter motherboards
- 316 Front-end Boards
- 16 Readout Controllers

- CRV identifies cosmic ray muons that produce conversion-like backgrounds
- Design driven by need for excellent efficiency, large area, small gaps, high background rates, access to electronics, and constrained space
- Technology: Four layers of extruded polystyrene scintillator counters with embedded wavelength shifting fibers, read out with SiPM photodetectors
- A track stub in at least 3/4 layers, localized in time+space produces a veto in offline analysis

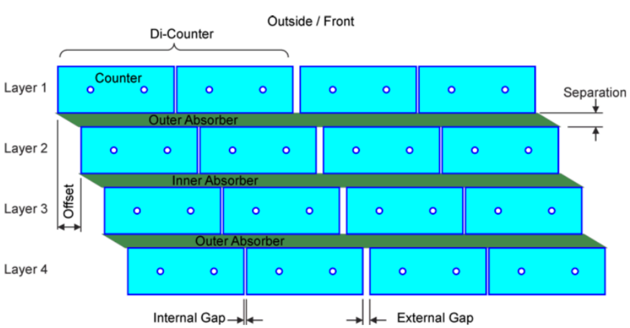

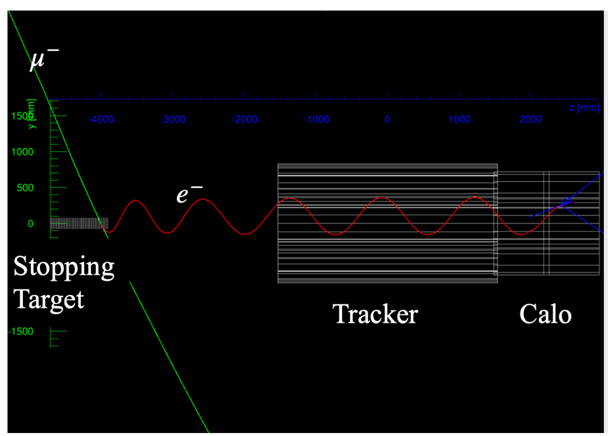

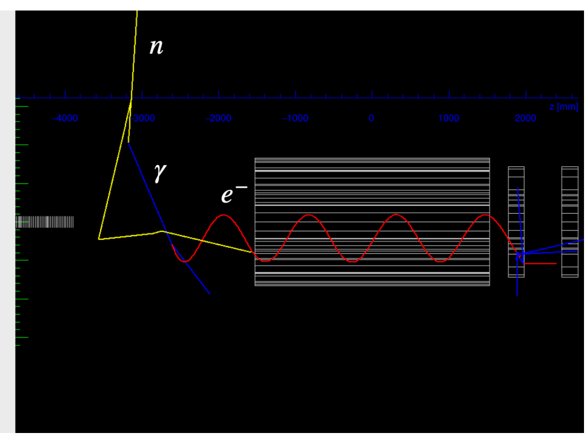

STM: to measure the stopped muon rate

- Captured muons normalize the cLFV measurement.
- Captured muons can emit characteristic Al X-rays.
- Captured muons are measured by reconstructing the ^{27}Al X-ray energy spectrum.
- Captured muons = 60.9% of Stopped muons

STM: Reconstructs ^{27}Al energy spectrum.

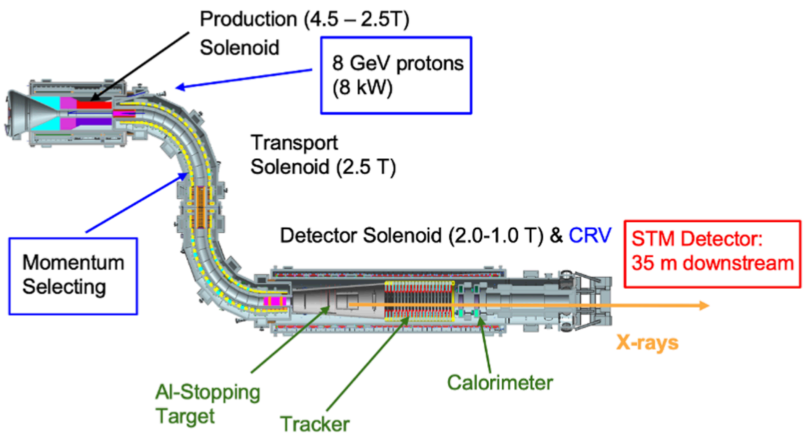

High Purity Germanium (HPGe) Detector.

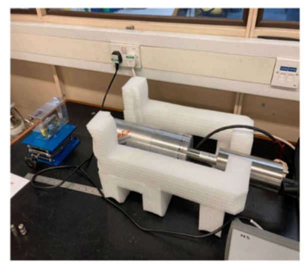

Corrected by STM acceptance

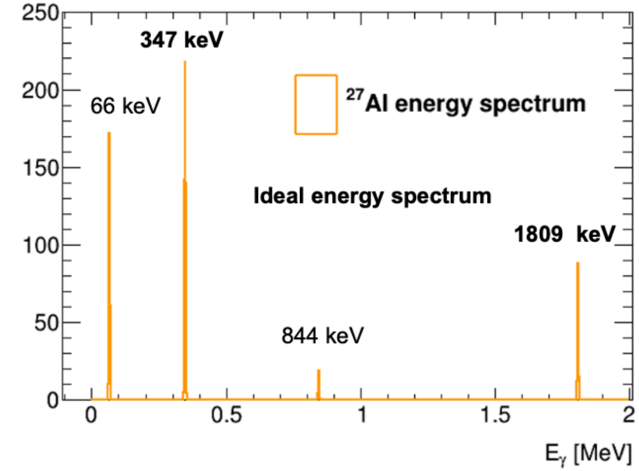

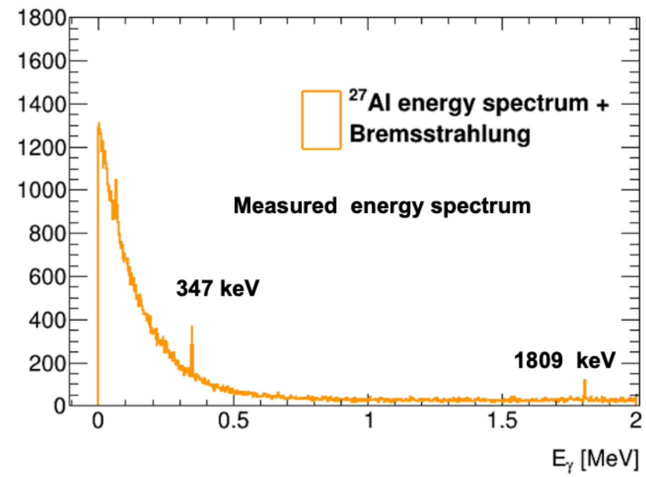

Mu2e/Mu2e-II Extinction

- Extinction is measure of out-of-time beam
- Mu2e-II requires extinction < 10^{-11}
  - cf Mu2e requirement < 10^{-10}
- Two factors contribute to extinction: intrinsic accelerator extinction, and AC resonant dipole sweepers
- Mu2e AC dipoles sweep away out-of-time protons into collimators– plan to use also for Mu2e-II
- PIP-II Linac extinction specification is 10^{-4-} -Likely will be better
- Expect improved performance from AC dipole for Mu2e-II (10^{-9} with safety margin)
  - Lower momentum means larger deflection
  - No beam halo from Mu2e's slow extraction septum
  - Lower momentum means lower punch through at collimator

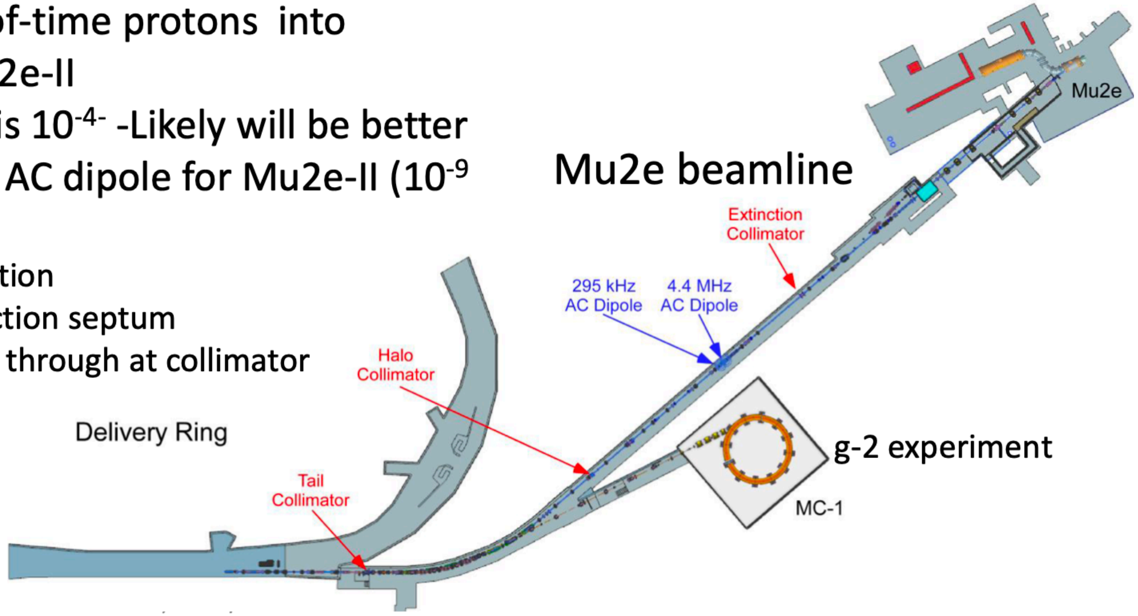

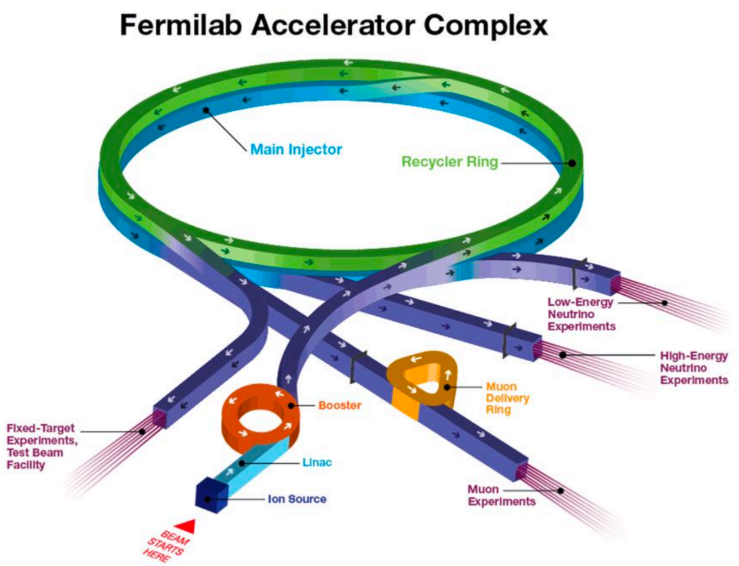

Mu2e: proton delivery

- get 0.4 s of pulsed beam per 1.4 s Booster cycle
- Delivery ring-storage ring
- Peel off small fraction of stored beam every cyclotron turn (period=1695 ns)
- Resonant extraction is considered challenging, therefore commissioning is commencing early (now)
- Mu2e has priority muon running for current run period to develop the proton beam line and extraction
- Run 1 (2026 before LBNF/PIP-II shutdown) will use the Booster and current Linac,
- Run 2, after shutdown, use new PIP-II Linac to inject into Booster

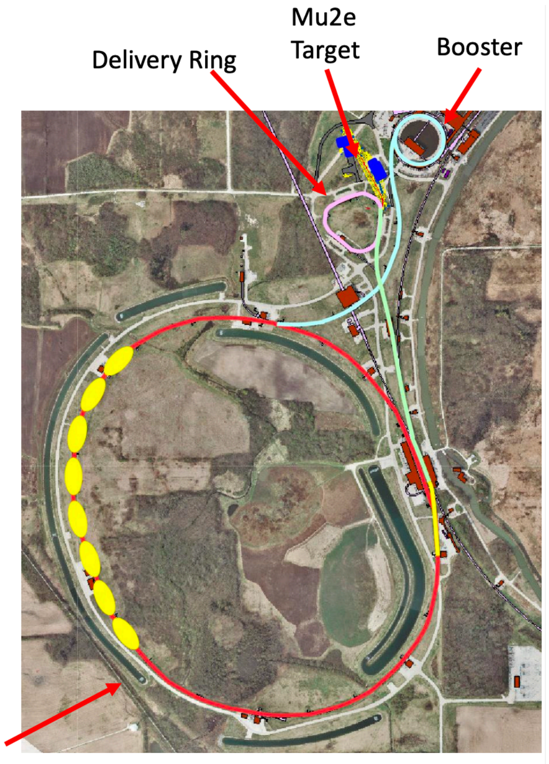

Schedules

- Mu2e

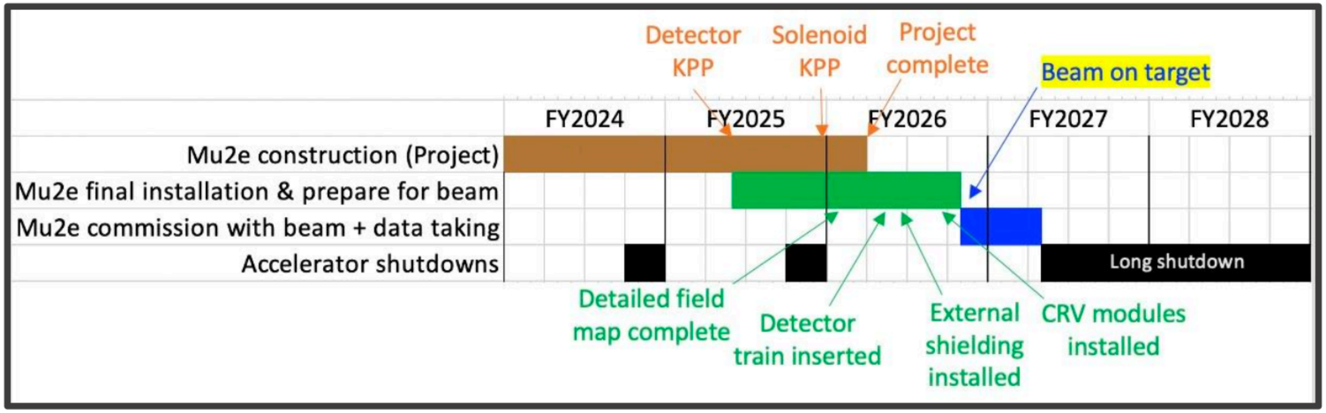

- Charged Lepton Flavor Tests

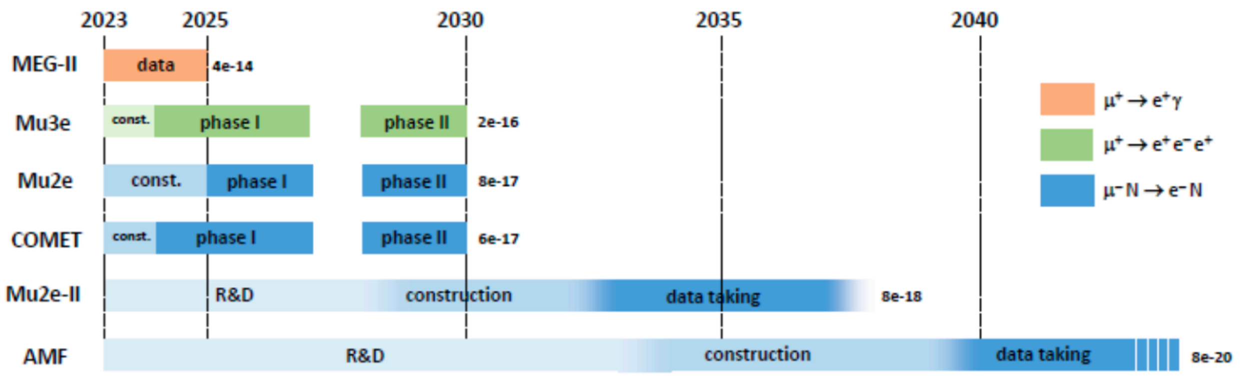

Table 1. Expected running time, proton counts, and stopped muon counts for Mu2e Run I. The running time is the time, in seconds, during which the experiment is running and taking data. The numbers in the last two columns do not include the trigger, reconstruction, and selection efficiency.

Running mode	Mean proton pulse intensity	Running time (s)	N(POT)	N(stopped muons)
Low intensity	1.6×10^7	9.5×10^6	2.9×10^{19}	4.6×10^{16}
High intensity	3.9×10^7	1.6×10^6	9.0×10^{18}	1.4×10^{16}
Total		11.1×10^6	3.8×10^{19}	6.0×10^{16}

3.1. Pileup Simulation

Electron events with $p_e \sim 100$ MeV/c are extremely rare. In addition to hits produced by signal-like particle, an event accepted by the Mu2e trigger is expected to have multiple background hits produced by lower momentum particles. Moreover, the Mu2e readout event window is about 1200 ns long, and a realistic detector simulation has to handle particles producing hits in the detector at different times. For the low intensity running mode with the mean intensity of 1.6×10^7 protons/pulse, about 25,000 muons per proton pulse stop in the Al stopping target. About 39% of muons decay in orbit, and about 61% are captured by the Al nuclei, so an average "zero bias" Mu2e event includes $\sim 10,000$ muon DIO and $\sim 15,000$ nuclear muon captures. For the high intensity mode, the corresponding numbers are about 2.5 times higher. The impact of the proton pulse intensity variations is taken into account by approximating them with the log-normal distribution with SDF = 60%. The simulated proton pulse intensity distributions for the low and high intensity running modes are shown in Figure 4. The highest simulated pulse intensity is 1.2×10^8 protons per pulse. The upper cutoff is taken into account in the evaluation of the systematic uncertainties.

Antiprotons are produced in the tungsten Production Target by the reaction:

$$p + W \longrightarrow (W^* + \bar{p}) + X \quad (1)$$

In the *Xsec frame* the production probability is flat in ϕ, while $\cos\theta$ and momentum (p) dependence is given by the inclusive differential cross section.

The basic underlying process is the well known reaction:

$$p + p \longrightarrow (p + \bar{p}) + p + p \quad (2)$$

The number of antiprotons produced in the production target ($N_{\bar{p}}^{PT}$) per POT is given by:

$$\frac{N_{\bar{p}}^{PT}}{POT} = \frac{\sigma_{\bar{p}}}{\sigma_{inelastic}} \frac{N_{inelastic}}{N_{POT}} = \frac{0.5 \times 0.2824\ mb}{1710\ mb} 0.792 = 6.5 \times 10^{-5} \quad (12)$$

where $\sigma_{\bar{p}}$ is the total antiproton production cross section obtained integrating the differential cross section in Eq. 11, $N_{inelastic}/N_{POT} = 0.792$ is the probability, obtained by Monte Carlo, that a proton in the beam produces an inelastic interaction in the tungsten target, and $\sigma_{inelastic} = 1710$ mb is taken from Ref. [58]. This value for the total proton inelastic cross section on tungsten is ~11% higher than the value of 1517 mb obtained with MCNP [59], but this discrepancy can be neglected with respect to the 100% error

A standard measure of an experiment's ability to make a discovery is its "median discovery potential" characterized by the minimal signal strength for which, given the mean background expectation μ_B, the probability to satisfy the discovery criterion would be at least 50% . Standard for HEP, a discovery is defined as a measurement yielding a significant, "5σ", deviation from the expected background with the probability

$$P < \int_5^\infty e^{-x^2/2}\, dx/\sqrt{2\pi} = 2.87 \times 10^{-7}$$

While this definition is very clear, it may not provide the best figure of merit for the sensitivity optimization. Due to the discrete nature of the measurement, the same number of events is needed to claim a discovery for a range of μ_B values. In this case, higher background values correspond to better sensitivities, which is rather counter-intuitive. A better figure of merit is the average discovery potential, defined as the signal strength that corresponds to an average 5σ deviation from the background-only hypothesis. Using the average discovery potential avoids the known pathologies of the median discovery potential – see the discussion by Bhattiprolu et al. comparing these and other methods of quoting the discovery potential [62]. It is also similar to the method proposed by Feldman and Cousins (FC), where the average of the distribution

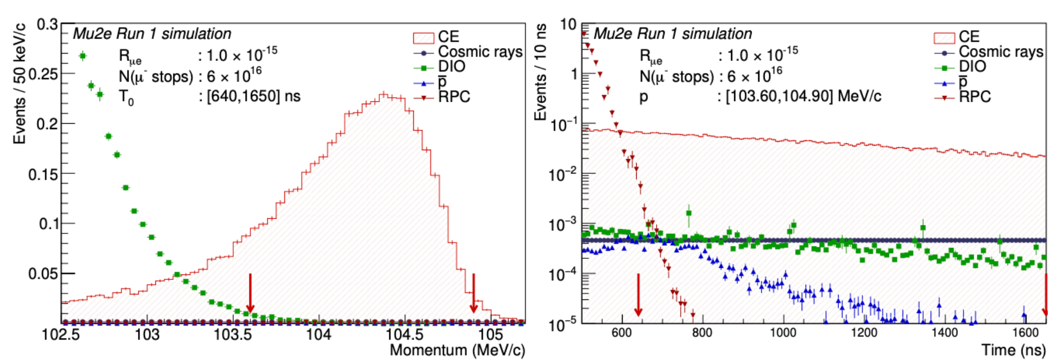

Datasets and code developed for the antiproton background study

- The generation of the $\overline{p}$s in the production target and tracing them from the Production to the Detector Solenoid was done using the Mu2e Offline software.

- A dataset containing the position and time of the stopped $\overline{p}$s at the ST from the SU 2020* work was the starting point of our study.

- A data sample with 10^4 pure $p\overline{p}$ annihilation events in the ST was created. Most of the reconstruction algorithm was developed based on the test results obtained with this pure $p\overline{p}$ data.

- Further, 10^4 $p\overline{p}$ annihilation events with low intensity (1.6×10^7 protons/pulse) and high intensity pile-up modes were generated as well.

- The simulation, digitisation and reconstruction fcl files can be found at https://github.com/Mu2e/pbar2m.

ϕ cluster finder algorithm

—- Muon —- Pion

ϕ cluster finder algorithm

- Input : Combo hits (or Time Clusters)

—- Muon —- Pion

ϕ cluster finder algorithm

- Input : Combo hits (or Time Clusters)
- Loop through the hits, fill the ϕ histogram.

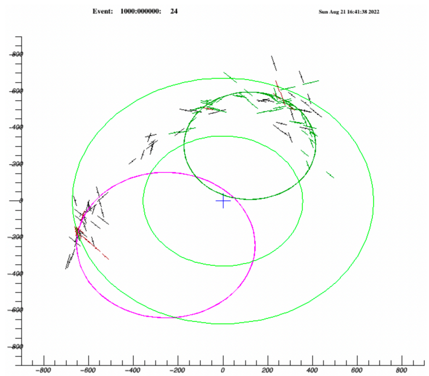

XY View

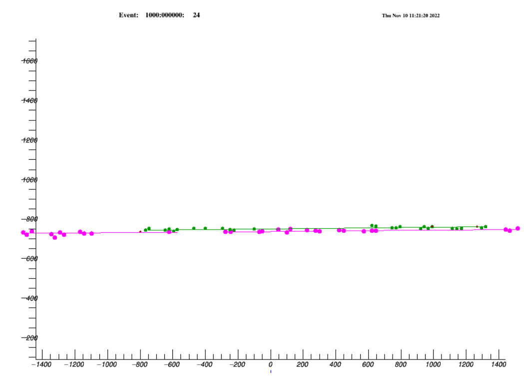

TZ view

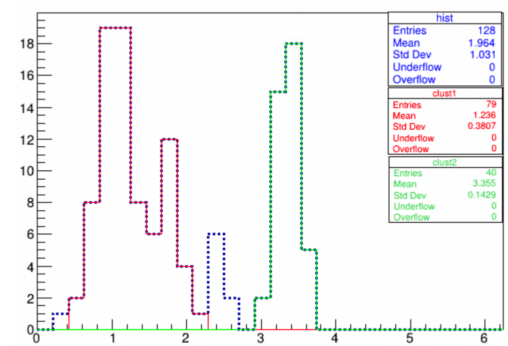

Event : 24 $\Delta\phi$ = 2.11854 rad

—- Muon —- Pion

ϕ cluster finder algorithm

- Input : Combo hits (or Time Clusters)
- Loop through the hits, fill the ϕ histogram.
- Find the peak bin and go through the bins around it with content > threshold.

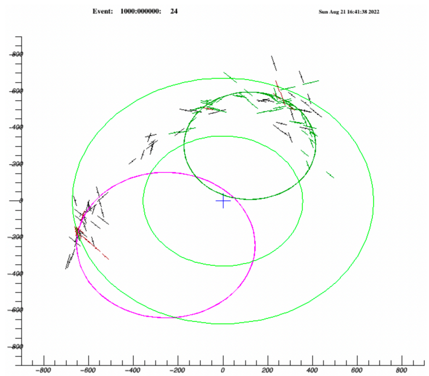

XY View

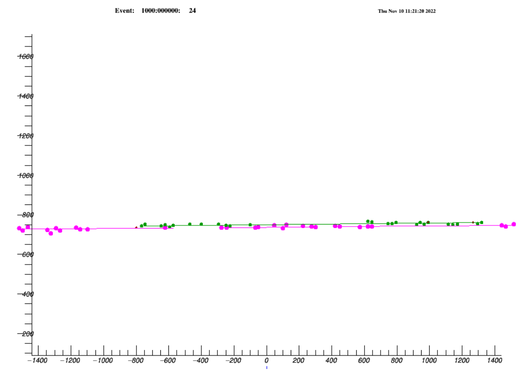

TZ view

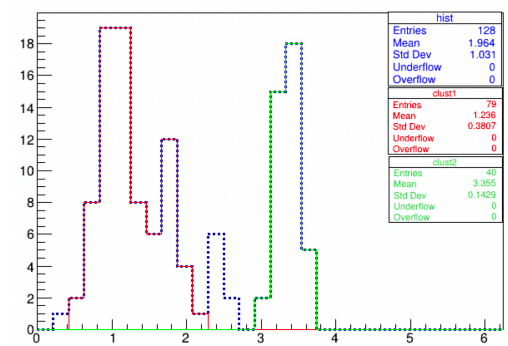

Event : 24 $\Delta\phi$ = 2.11854 rad

—- Muon —- Pion

ϕ cluster finder algorithm

- Input : Combo hits (or Time Clusters)
- Loop through the hits, fill the ϕ histogram.
- Find the peak bin and go through the bins around it with content > threshold.
- This gives ϕ_{min} and ϕ_{max} for a cluster.

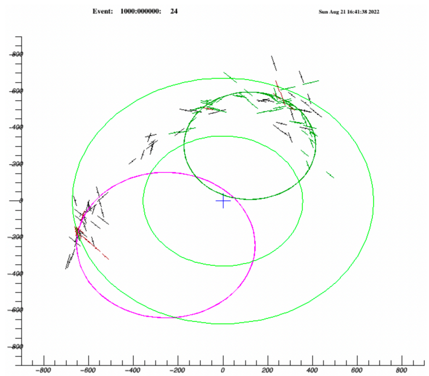

XY View

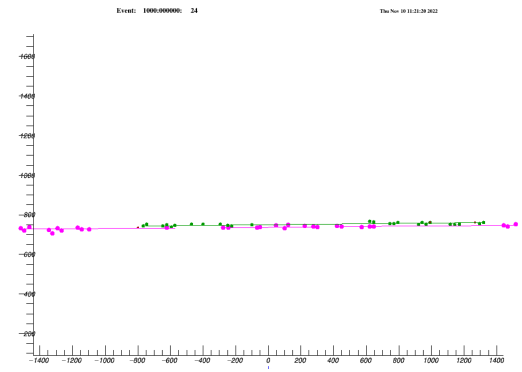

TZ view

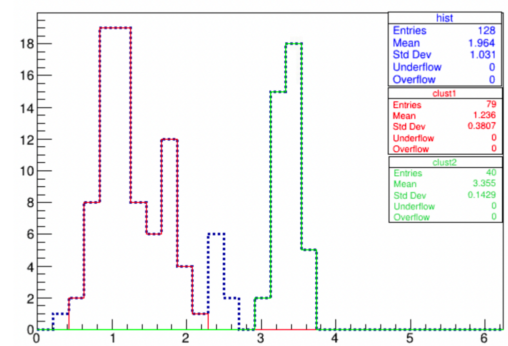

Event : 24 $\Delta\phi$ = 2.11854 rad

—- Muon —- Pion

ϕ cluster finder algorithm

- Input : Combo hits (or Time Clusters)
- Loop through the hits, fill the ϕ histogram.
- Find the peak bin and go through the bins around it with content > threshold.
- This gives ϕ_{min} and ϕ_{max} for a cluster.
- Loop through the hits and flag the hits with ϕ between ϕ_{min} and ϕ_{max} as “UsedHits”. These hits form one cluster.

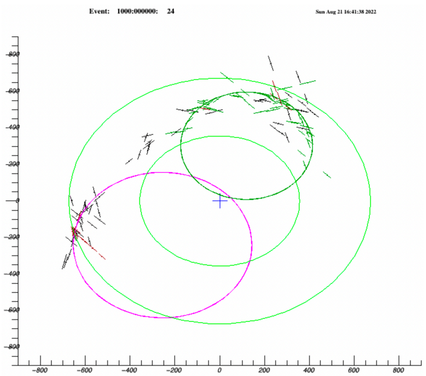

XY View

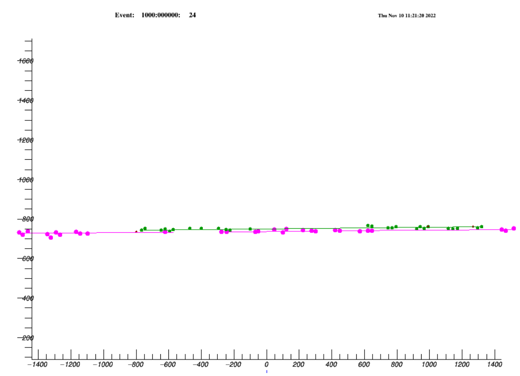

TZ view

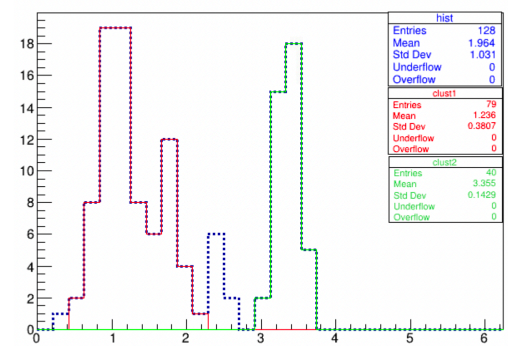

Event : 24 $\Delta\phi$ = 2.11854 rad

—- Muon —- Pion

ϕ cluster finder algorithm

- Input : Combo hits (or Time Clusters)
- Loop through the hits, fill the ϕ histogram.
- Find the peak bin and go through the bins around it with content > threshold.
- This gives ϕ_{min} and ϕ_{max} for a cluster.
- Loop through the hits and flag the hits with ϕ between ϕ_{min} and ϕ_{max} as “UsedHits”. These hits form one cluster.
- Repeat the above procedure for the rest of the hits which are not “UsedHits”.

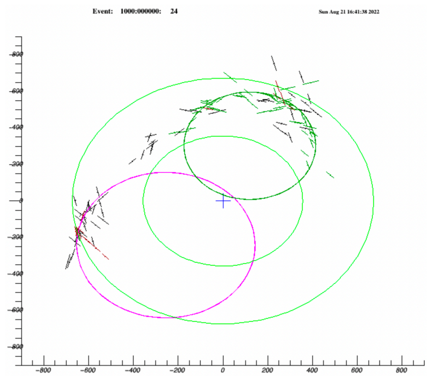

XY View

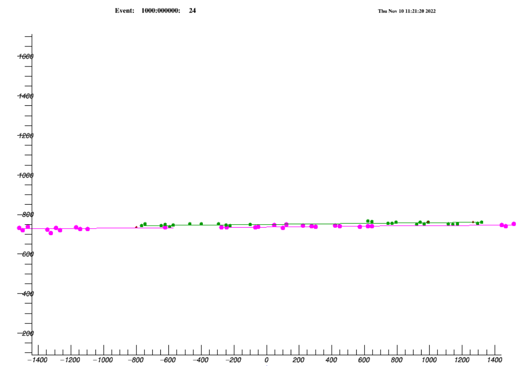

TZ view

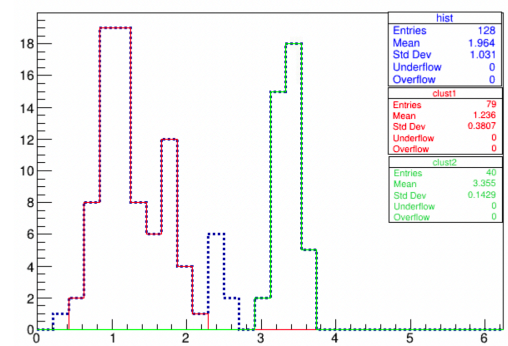

Event : 24 $\Delta\phi$ = 2.11854 rad

—- Muon —- Pion

ϕ cluster finder algorithm

- Input : Combo hits (or Time Clusters)
- Loop through the hits, fill the ϕ histogram.
- Find the peak bin and go through the bins around it with content > threshold.
- This gives ϕ_{min} and ϕ_{max} for a cluster.
- Loop through the hits and flag the hits with ϕ between ϕ_{min} and ϕ_{max} as “UsedHits”. These hits form one cluster.
- Repeat the above procedure for the rest of the hits which are not “UsedHits”.
- Form time clusters (algorithm borrowed from the present Offline TimeClusterFinder) from the hits of a ϕ cluster.

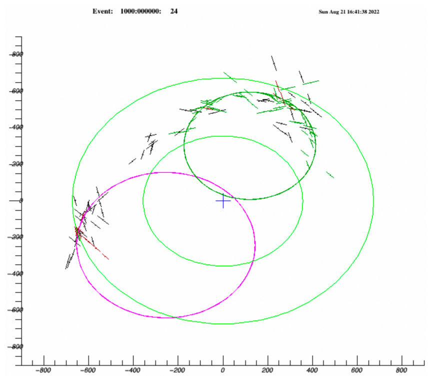

XY View

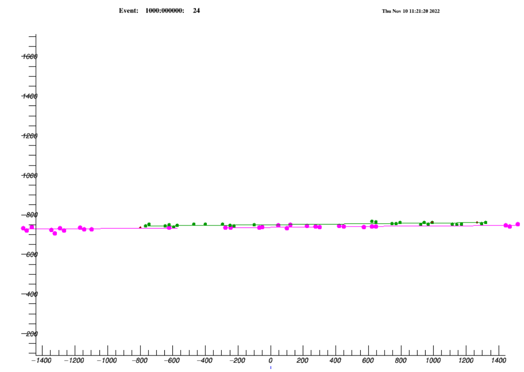

TZ view

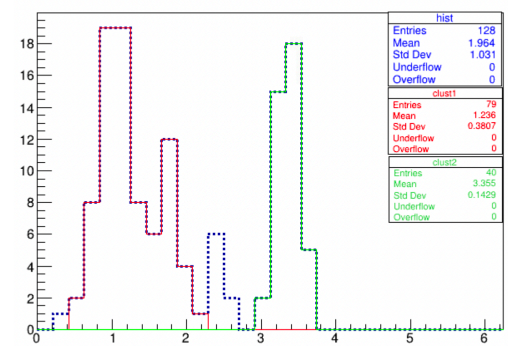

Event : 24 $\Delta\phi$ = 2.11854 rad

—- Muon —- Pion

ϕ cluster finder algorithm

- Input : Combo hits (or Time Clusters)
- Loop through the hits, fill the ϕ histogram.
- Find the peak bin and go through the bins around it with content > threshold.
- This gives ϕ_{min} and ϕ_{max} for a cluster.
- Loop through the hits and flag the hits with ϕ between ϕ_{min} and ϕ_{max} as “UsedHits”. These hits form one cluster.
- Repeat the above procedure for the rest of the hits which are not “UsedHits”.
- Form time clusters (algorithm borrowed from the present Offline TimeClusterFinder) from the hits of a ϕ cluster.
- If the time cluster has > 10 straw hits, add it to the event.

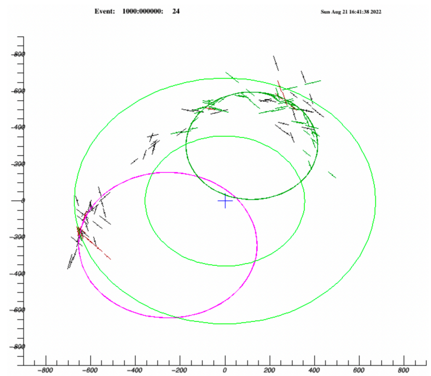

XY View

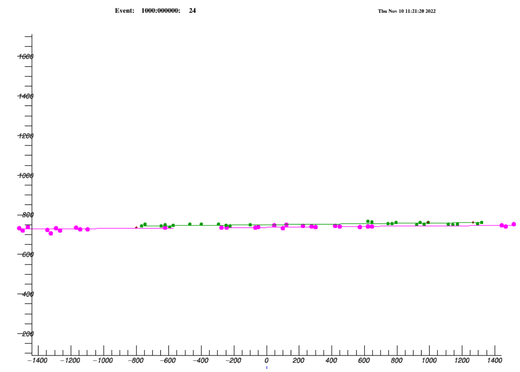

TZ view

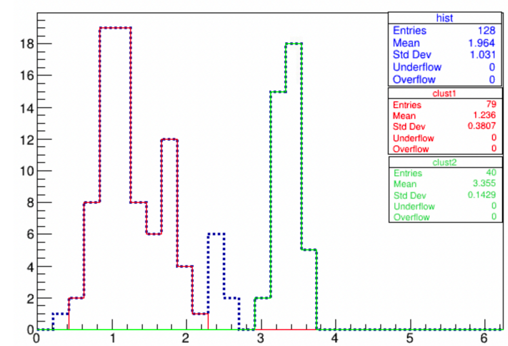

Event : 24 $\Delta\phi$ = 2.11854 rad

—- Muon —- Pion

$\Delta\phi$ distribution for single interaction $p\bar{p}$ annihilation events

- The events with two output time clusters after the PhiClusterFinder stage were used to fill the above histogram.

$$\Delta\phi = \phi_1 - \phi_2$$

- Studying the $\Delta\phi$ distributions we decided to set a $\Delta\phi_{min} = 1.5$ rad cut to select events for the two tracks per event reconstruction.

$\Delta\phi$ distribution for single interaction $p\bar{p}$ annihilation events

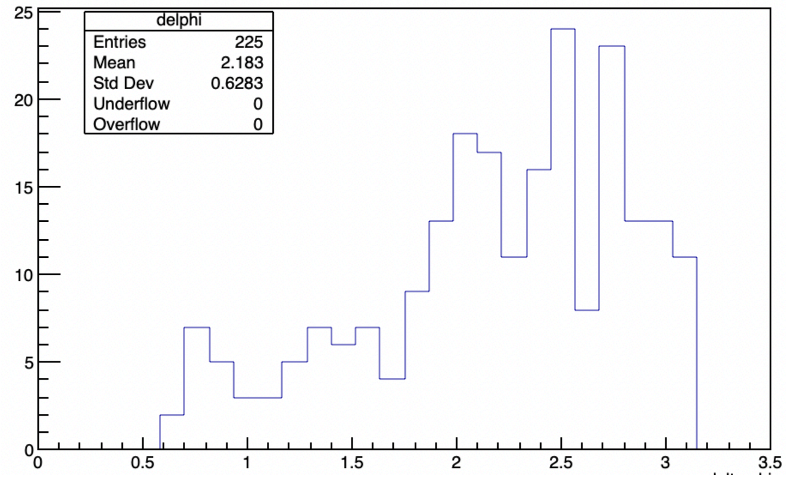

$\Delta\phi$

$p\bar{p}$ data sample (10^4 generated events)

- The events with two output time clusters after the PhiClusterFinder stage were used to fill the above histogram.

$$\Delta\phi = \phi_1 - \phi_2$$

- Studying the $\Delta\phi$ distributions we decided to set a $\Delta\phi_{min} = 1.5$ rad cut to select events for the two tracks per event reconstruction.

Default Mu2e Offline v/s New Reconstruction workflow

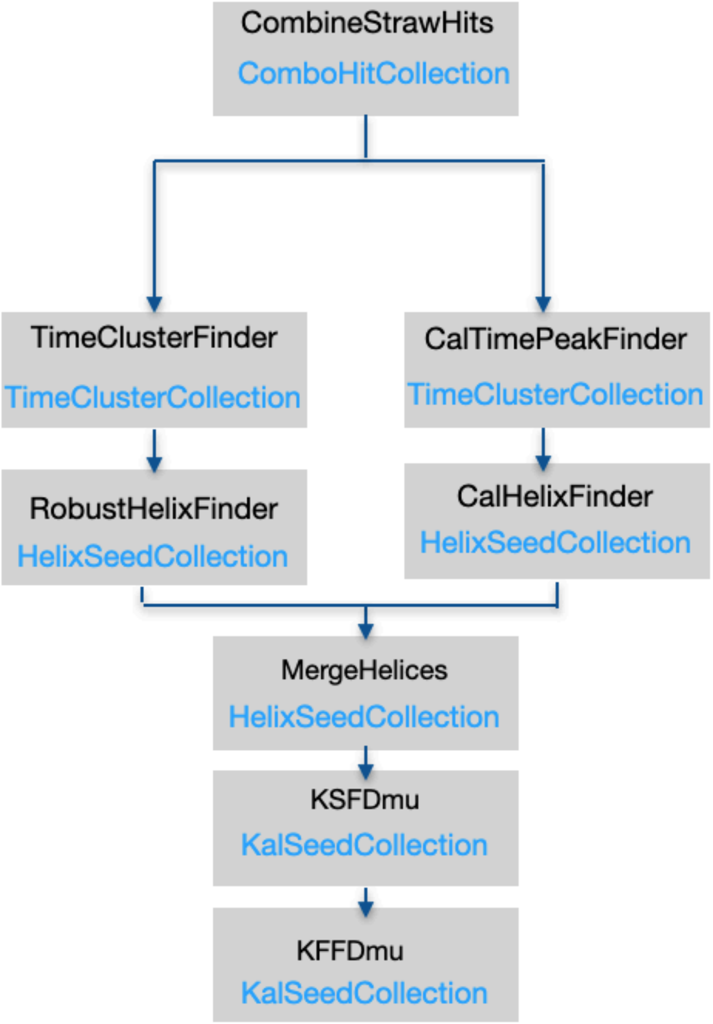

Default reconstruction chain

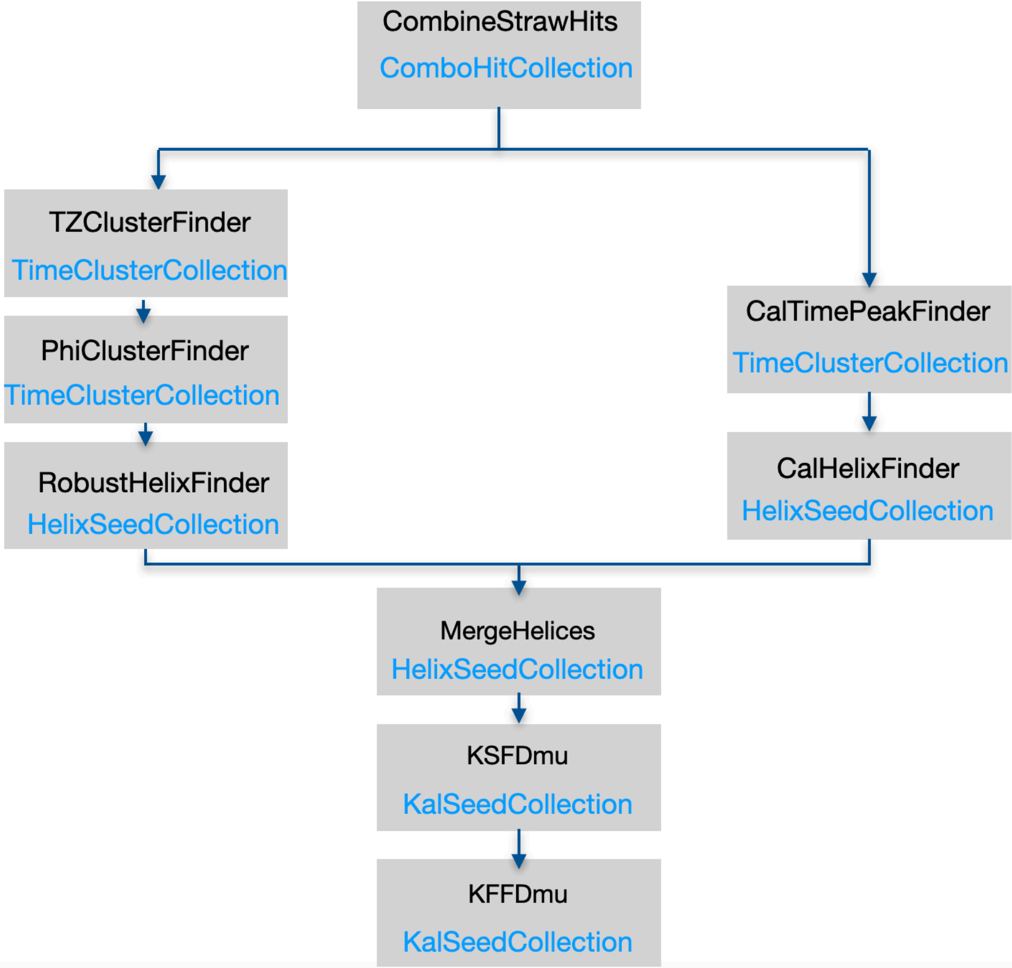

New Reconstruction chain using the DeltaFinder, TZFinder and PhiClusterFinder

Δt between the tracks of two-track events

- Given here are the Δt distributions for two-track final state $p\overline{p}$ annihilation events where each reconstructed track has a momentum > 80 MeV/c.
- Tracks from the same $p\overline{p}$ interaction could be close in time, but could also be up to 100 ns apart.
- The events with track hits separated in time make different time clusters.

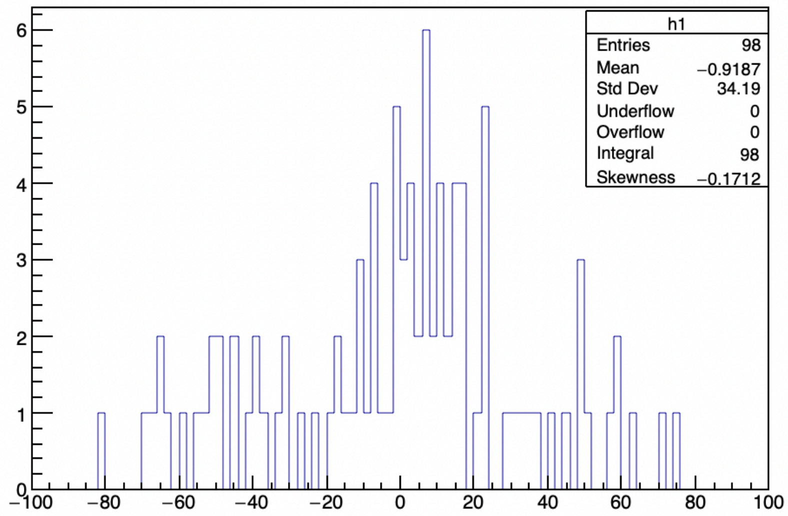

Δt (ns) (Pure $p\overline{p}$ events)

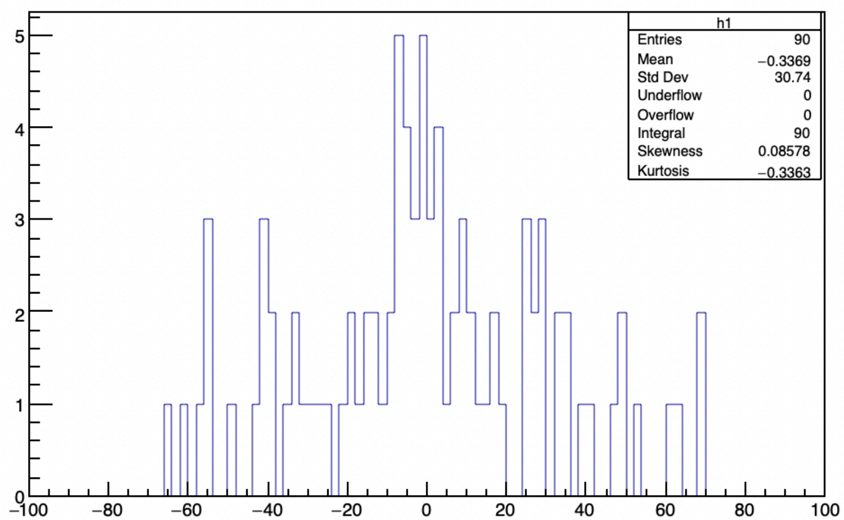

Δt (ns) ($p\overline{p}$ + 1BB pile-up events)

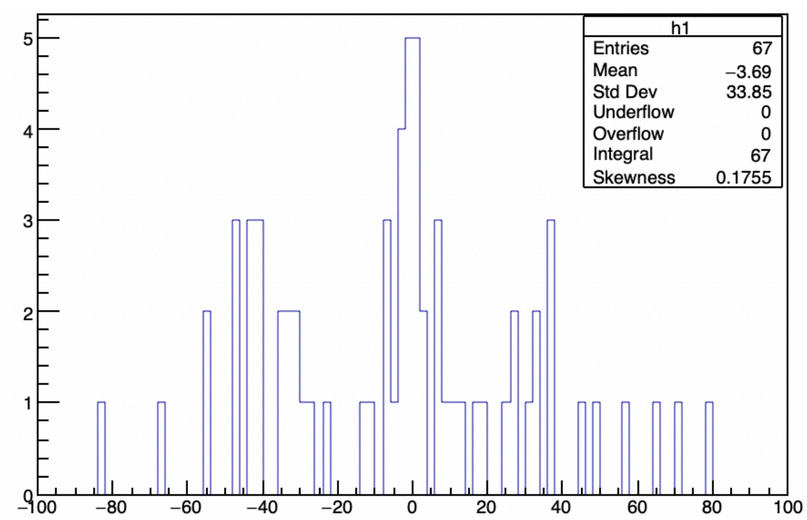

Δt (ns) ($p\overline{p}$ + 2BB pile-up events)

Some examples of two-track events with large Δt between the particle tracks

Event: 527

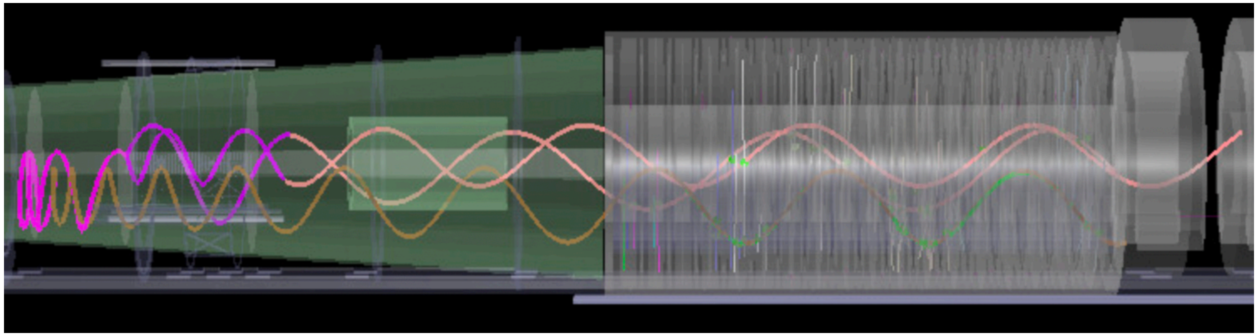

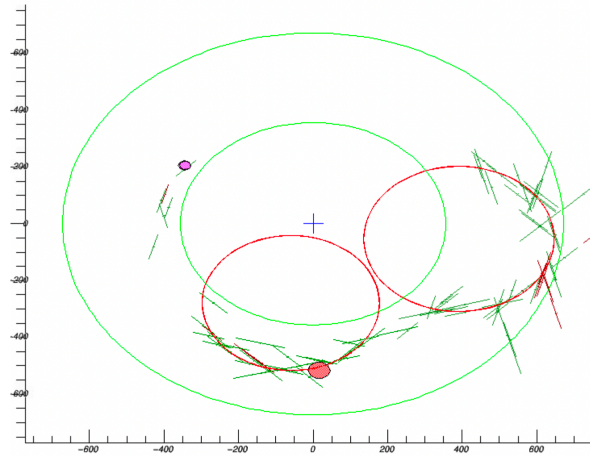

$\Delta t = 63ns$

track 1 = μ^+, track 2 = $\mu-$

Event: 676

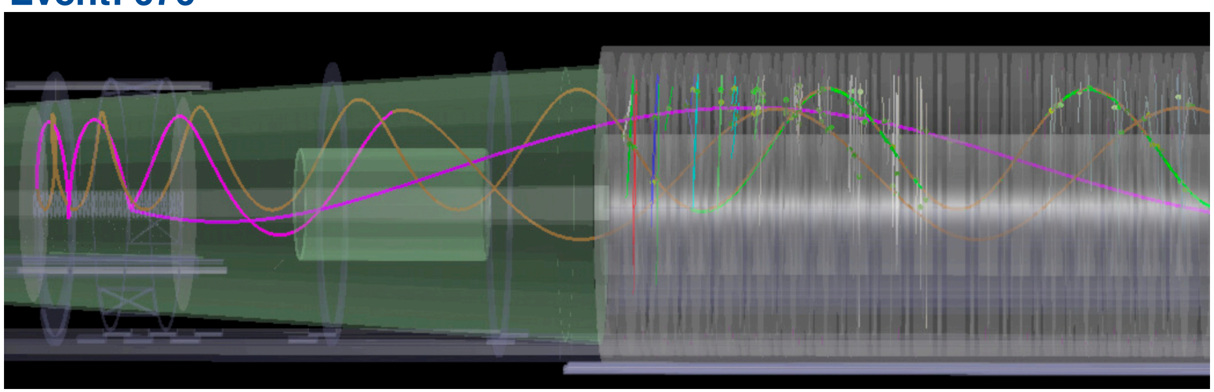

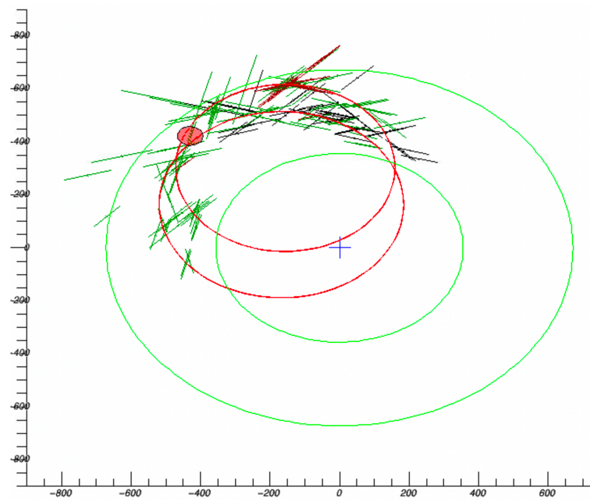

$\Delta t = 32ns$

track 1 = μ^-, track 2 = $\mu-$

XY view

$p\overline{p}$ annihilation event with two reconstructed tracks
Green = Muon, Pink = Pion in 3-D view
Red = Reconstructed track in 2-D view

Results with the single interaction $p\bar{p}$ annihilation at the ST events

Events with	0	1	2	3	4	5
Sim	7405	2159	381	50	4	1
TimeCluster	7913	1871	194	14	7	1
Helix	8287	1596	110	5	2	
Track	8702	1250	46	2		

$p\bar{p}$ data with default Offline workflow

Events with	0	1	2	3	4	5
Sim	7405	2159	381	50	4	1
TimeCluster	7913	1871	194	14	7	1
Phi	8036	1685	244	23	10	1
Helix	8349	1508	132	10	1	
Track	8791	1152	55	2		

$p\bar{p}$ data with FlgBkgHits -> TimeClusterFinderDmu -> New PhiCusterFinder -> HelixFinder

Events with	0	1	2	3	4	>=5
Sim	7405	2159	381	50	4	1
TZ	7120	2564	284	23	4	
Phi	7276	2229	416	47	27	5
Helix	7677	2007	289	23	4	
Track	8187	1680	128	4	4	1

$p\bar{p}$ data with DeltaFinder -> TZFinder -> New PhiCusterFinder -> HelixFinder

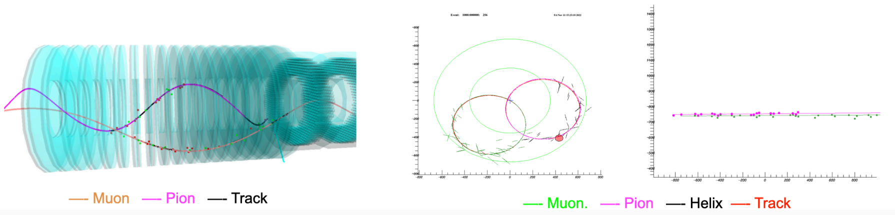

3-D and 2-D XY, tZ displays of an event with two reconstructed tracks

- Tested on 10^4 pure $p\bar{p}$ annihilation events.
- A sim particle is defined as a particle making at least 20 straw hits in the Tracker and having a momentum > 40 MeV/c. In this sample, there are 381 events with two particles each.
- The tables compare the number of events at each stage of reconstruction using the default and new chains of reconstruction
- The number of events with two helices increased from 110 to 289, number of events with two reconstructed tracks per event increased from 46 to 128 with the new reconstruction chain.

SimParticles

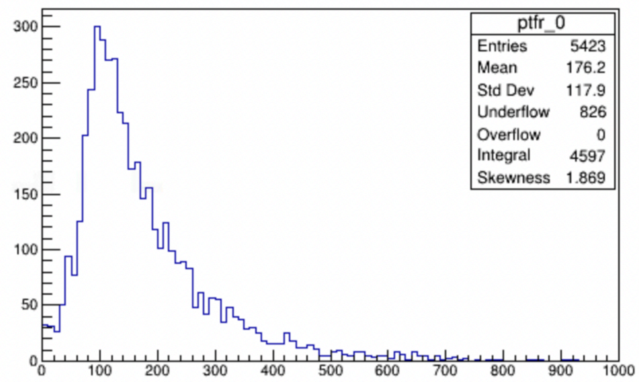

Momentum(MeV/c) at VD 13

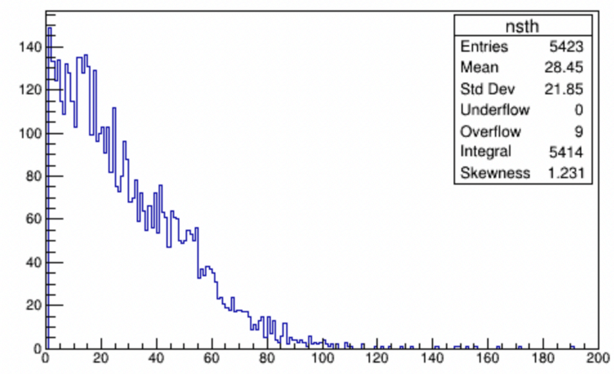

N straw hits

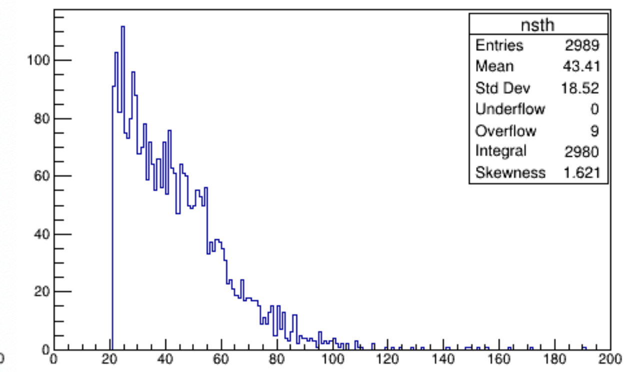

N straw hits

- 2150 events with 1 sim particle having > 20 straw hits
- 364 events with 2 sim particles each having > 20 straw hits
- 50 events with 3 sim particles.
- But only 1252 events pass the TC filter of the standard TPR trigger path.

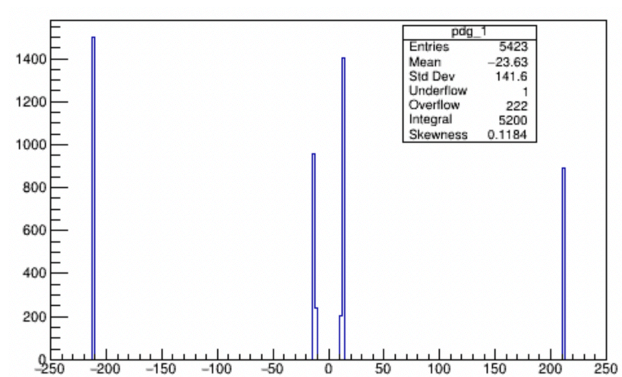

PDG code

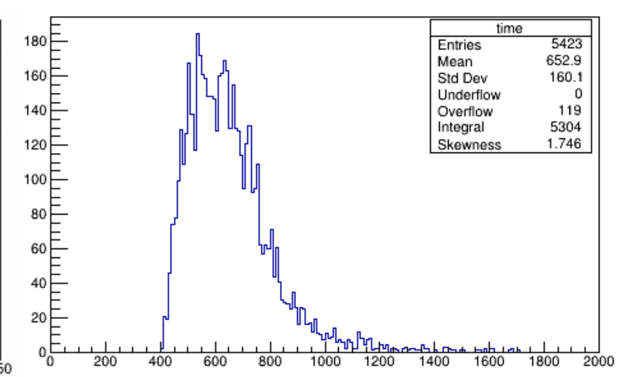

Time (ns)

All Helices

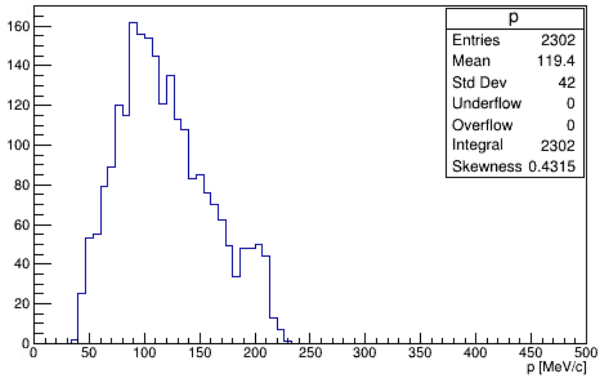

Total momentum (MeV/c)

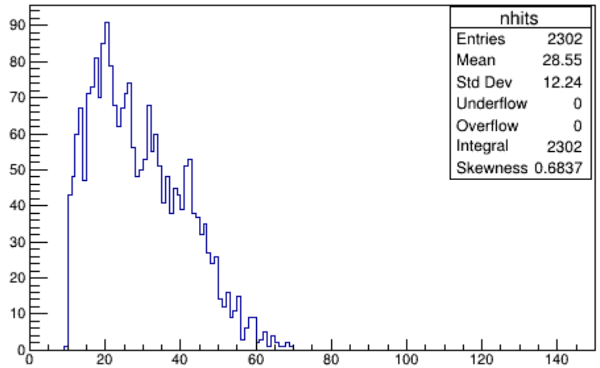

N straw hits

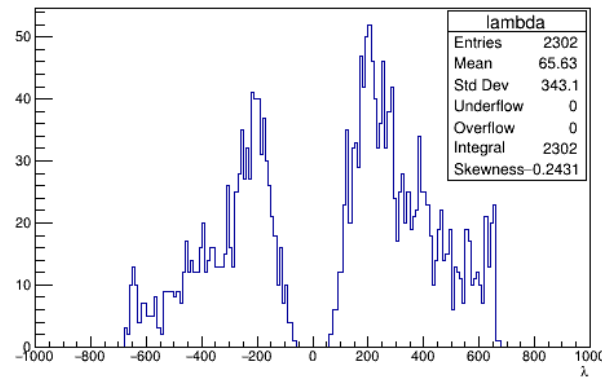

Lambda

- 1978 events with 1 helix
- 133 events with 2 helices
- 50 events with 3 sim particles.
- But only 345 events pass the HS filter of the standard TPR trigger path.

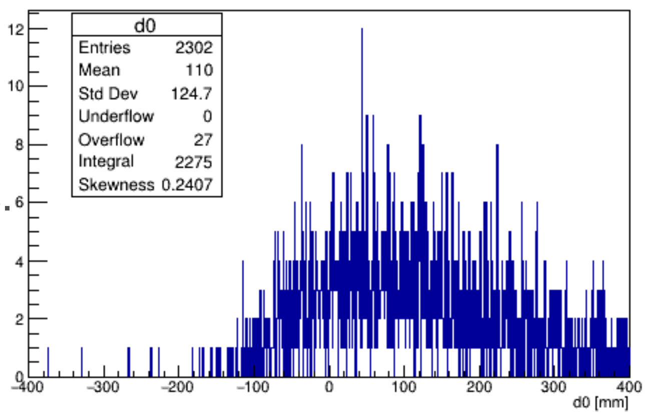

D0

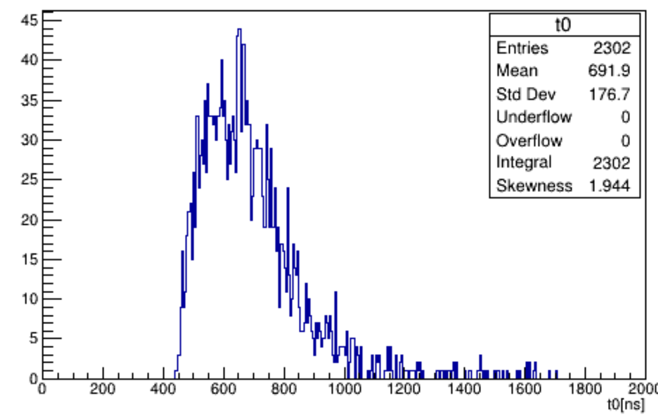

T0

Preliminary results with the single interaction $p\bar{p}$ annihilation at the ST events

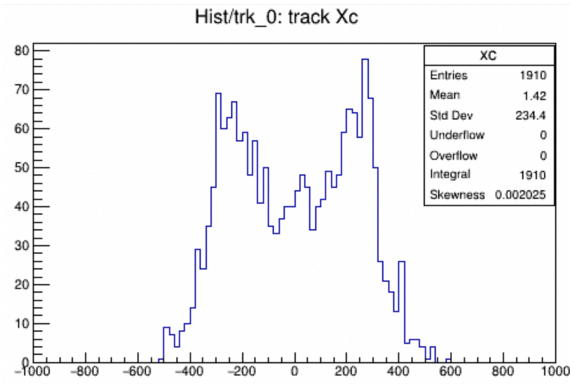

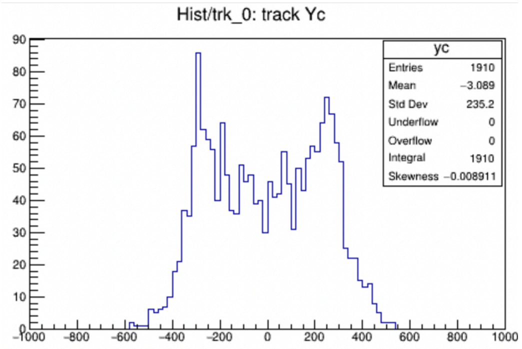

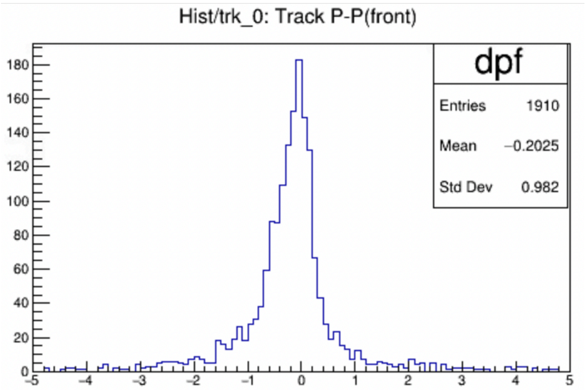

Momentum resolution

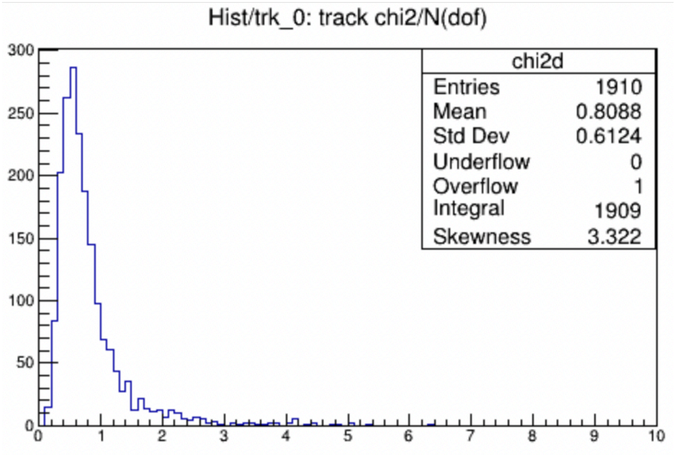

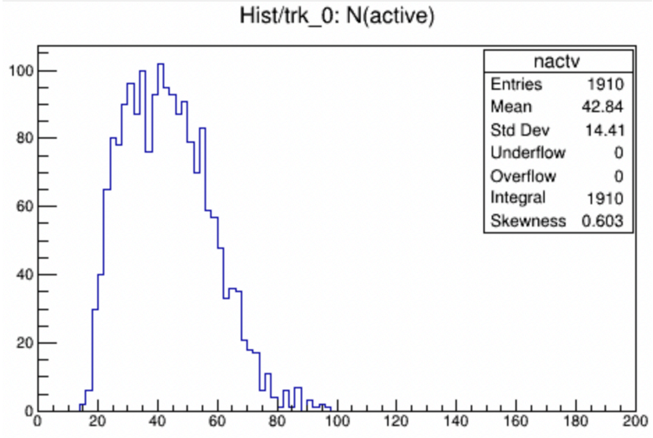

Straw hits

$p\bar{p}$ annihilation + pileup data samples

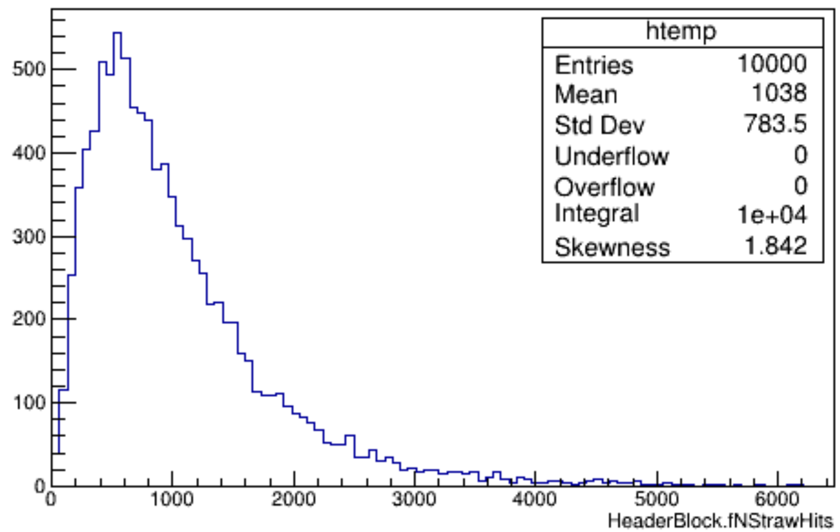

Number of Straw Hits
$p\bar{p}$ + 1BB data sample

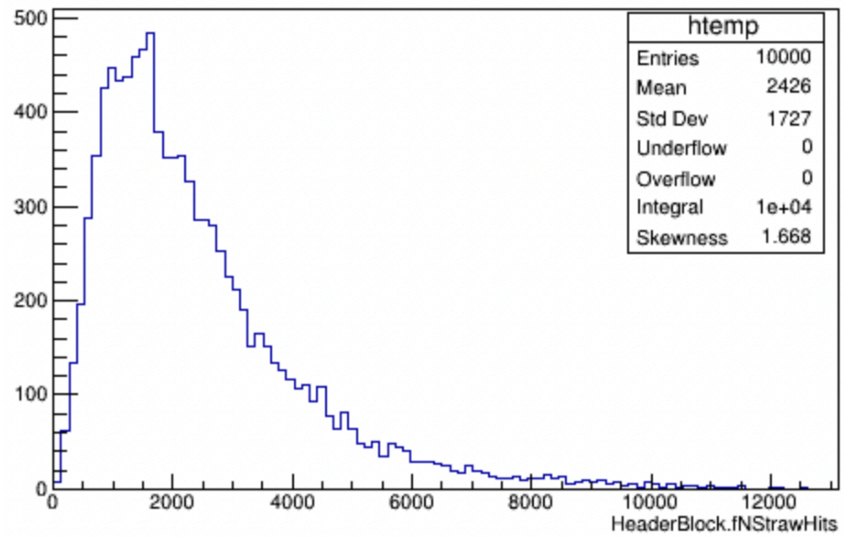

Number of Straw Hits
$p\bar{p}$ + 2BB data sample

- Mu2e Run I will operate in a low intensity mode: mean intensity of 1.6×10^7 protons per pulse, $\sim 25{,}000$ muons per pulse stop in the ST.
- For the high intensity mode, the corresponding numbers are about 2.5 times higher.
- We have generated 10^4 $p\bar{p}$ annihilation + low intensity (1BB) and high intensity (2BB) pileup data samples respectively.
- The number of straw hits per event are as expected for a data sample with pile-up.

Some cosmics multi-track events

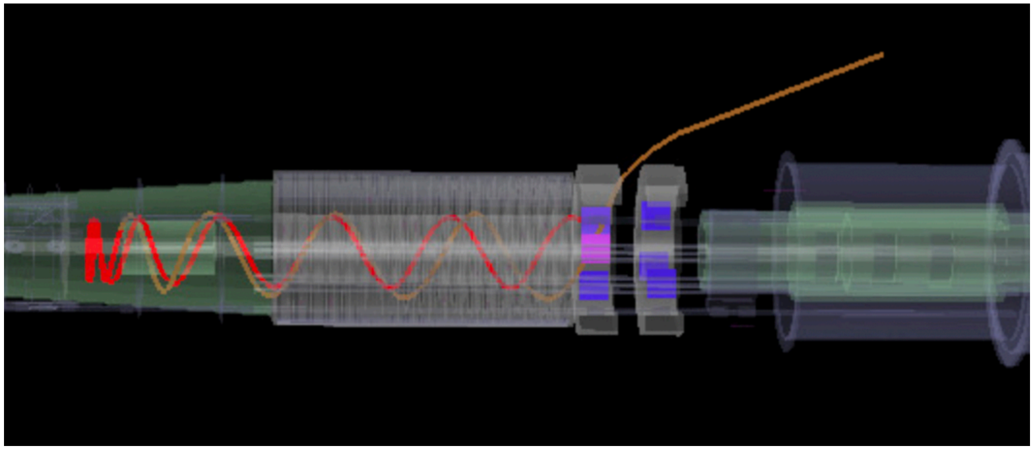

3-D view

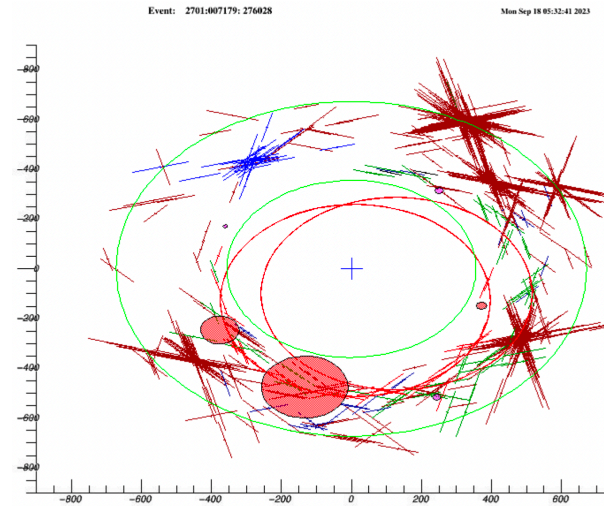

XY view

Green/Brown: Muon, Red Hit: Electron, Red Line: Reconstructed track

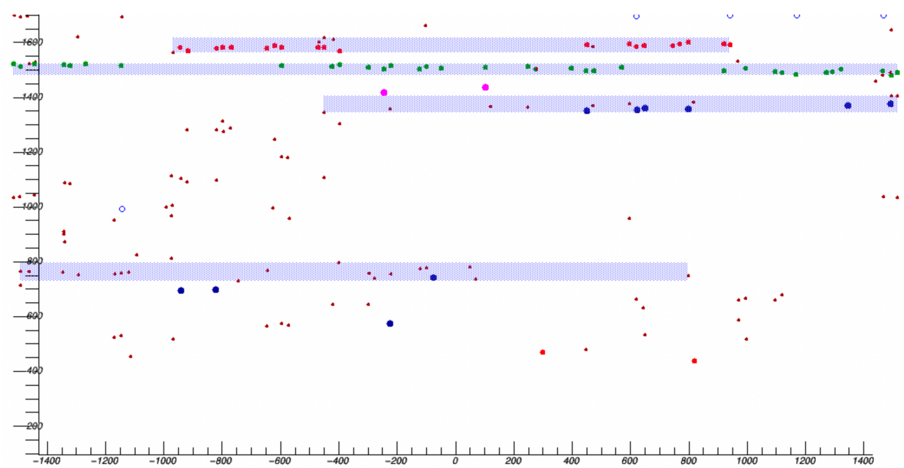

tZ view

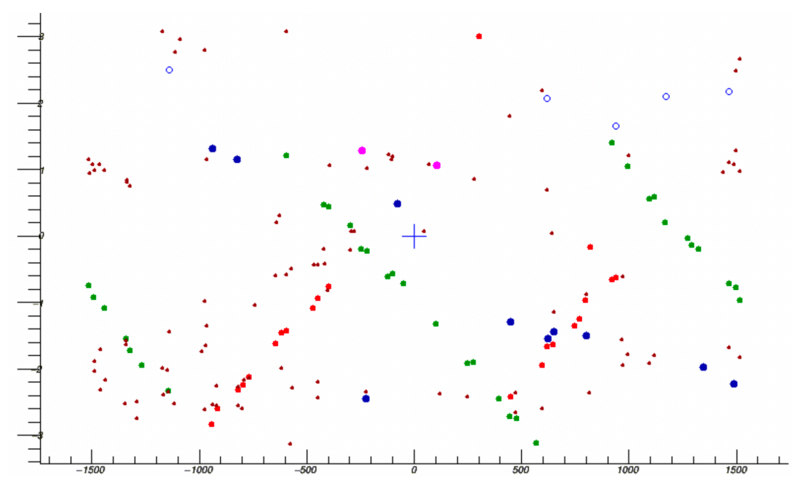

ϕZ view

Some cosmics multi-track events

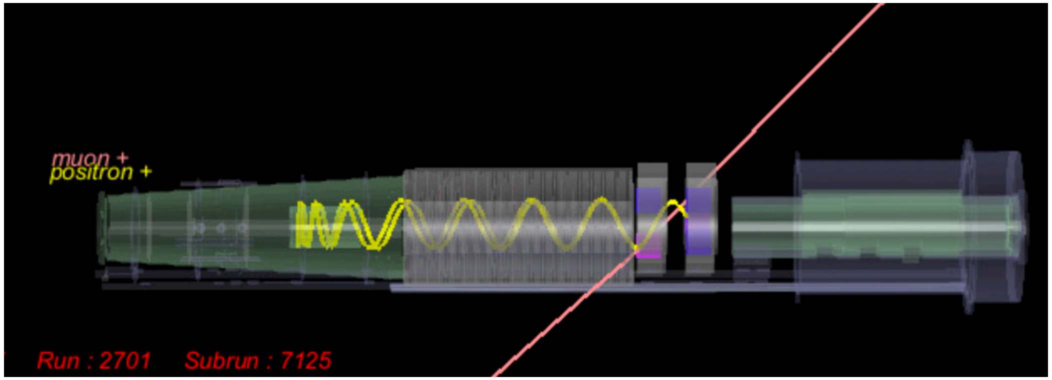

3-D view

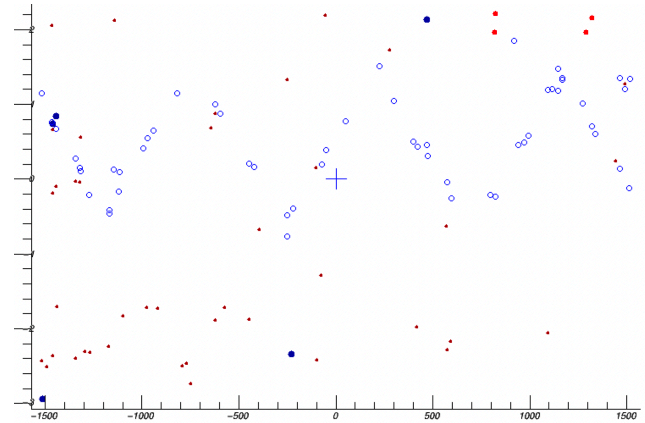

ϕZ view

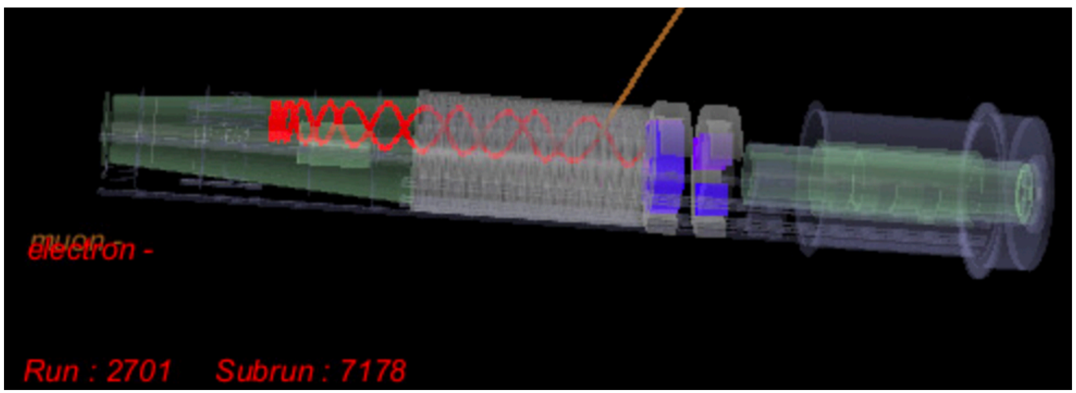

3-D view

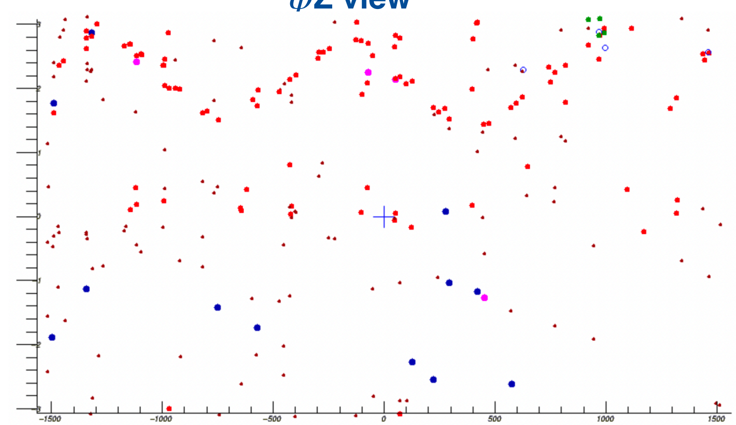

ϕZ view

Many cosmics 2-track events have 1 upstream and 1 downstream track.

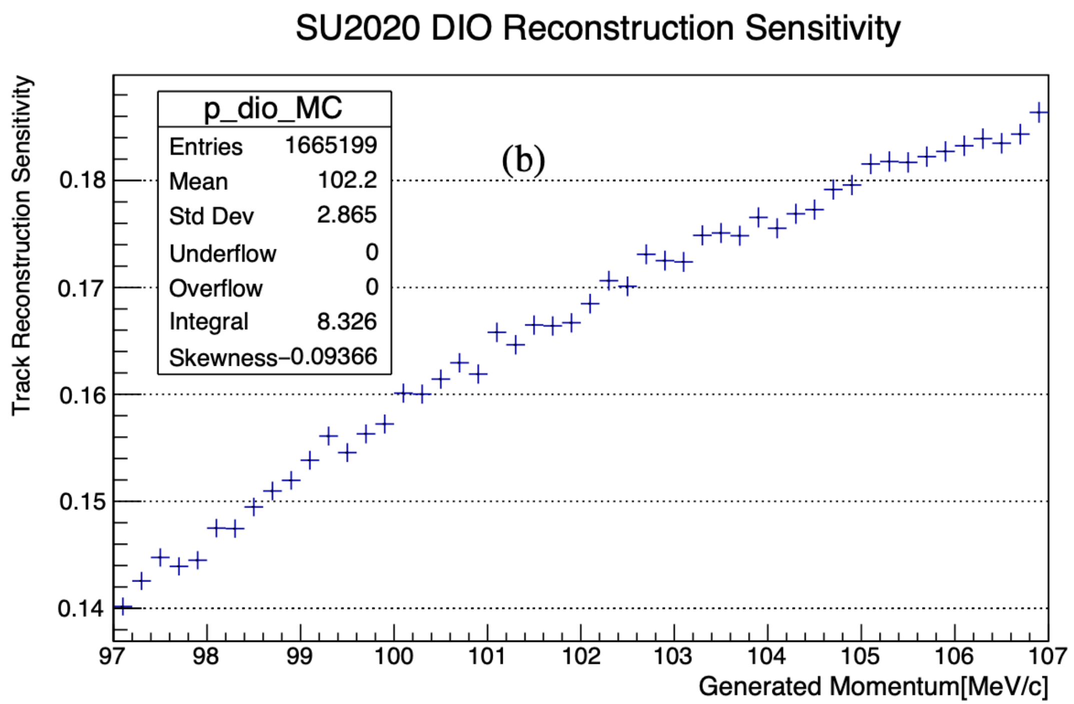

Track reconstruction efficiency, defined as the ratio of the number of single electron events with tracks passing all selections over the number of generated events, is a function of the track momentum